

Published in final edited form as:

Nat Rev Phys. 2021 December ; 3(12): 777–790. doi:10.1038/s42254-021-00368-5.

## Physics and biomedical challenges of cancer therapy with accelerated heavy ions

Marco Durante<sup>1,2,✉</sup>, Jürgen Debus<sup>3,4</sup>, Jay S. Loeffler<sup>5,6</sup>

<sup>1</sup>Biophysics Department, GSI Helmholtzzentrum für Schwerionenforschung, Darmstadt, Germany

<sup>2</sup>Institute of Condensed Matter Physics, Technische Universität Darmstadt, Darmstadt, Germany

<sup>3</sup>Department of Radiation Oncology and Heidelberg Ion Beam Therapy Center, Heidelberg University Hospital, Heidelberg, Germany

<sup>4</sup>German Cancer Research Center (DKFZ), Heidelberg, Germany

<sup>5</sup>Departments of Radiation Oncology and Neurosurgery, Massachusetts General Hospital, Boston, MA, USA

<sup>6</sup>Harvard Medical School, Boston, MA, USA

### Abstract

Radiotherapy should have low toxicity in the entrance channel (normal tissue) and be very effective in cell killing in the target region (tumour). In this regard, ions heavier than protons have both physical and radiobiological advantages over conventional X-rays. Carbon ions represent an excellent combination of physical and biological advantages. There are a dozen carbon-ion clinical centres in Europe and Asia, and more under construction or at the planning stage, including the first in the USA. Clinical results from Japan and Germany are promising, but a heated debate on the cost-effectiveness is ongoing in the clinical community, owing to the larger footprint and greater expense of heavy ion facilities compared with proton therapy centres. We review here the physical basis and the clinical data with carbon ions and the use of different ions, such as helium and oxygen. Research towards smaller and cheaper machines with more effective beam delivery

---

✉ M.Durante@gsi.de .

#### Author contributions

M.D. produced the first draft. J.D. and J.S.L. worked on the biological and clinical sections. All authors edited and modified the manuscript.

#### Competing interests

M.D. has no conflict of interest. J.S.L. is co-chair of the medical advisory board at Mevion. J.D. received grants from several companies and attended advisory board meetings of Merck KGaA (Darmstadt).

#### Peer review information

*Nature Reviews Physics* thanks Hywel Owen, Eleanor Blakely and the other, anonymous, reviewer(s) for their contribution to the peer review of this work.

#### Publisher's note

Springer Nature remains neutral with regard to jurisdictional claims in published maps and institutional affiliations.

#### Review criteria

The authors searched PubMed and Scopus using the keywords 'heavy ions', 'carbon ions', 'clinical trials' and 'comparative', and selected the period from 2016, considering our previous reviews on the topic<sup>21,83</sup>. We also searched the [ClinicalTrials.gov](https://www.clinicaltrials.gov) website with the keywords 'heavy ions', 'carbon ions', 'comparative', 'randomized' and 'phase III'. The website [www.ptcog.ch](http://www.ptcog.ch) was used for the latest statistics on particle therapy.

is necessary to make particle therapy affordable. The potential of heavy ions has not been fully exploited in clinics and, rather than there being a single ‘silver bullet’, different particles and their combination can provide a breakthrough in radiotherapy treatments in specific cases.

---

Radiotherapy with photons started shortly after the discovery of X-rays, but, as early as 1946, Robert R. Wilson proposed using accelerated charged particles—instead. The motivation for doing so was the Bragg peak of charged particles, that is, a plot of energy loss versus distance travelled through matter (the Bragg curve) shows a distinct peak before the particles come to rest (FIG. 1), suggesting that charged particles would be more conformal and produce lower toxicity to normal tissue than photons<sup>1</sup>. Wilson’s proposal involved protons, but the use of heavier ions in cancer therapy was proposed and pursued at Lawrence Berkeley Laboratory (LBL) by Cornelius A. Tobias<sup>2</sup>, with the idea that heavier ions have radiobiological properties that can lead to better tumour control than X-rays or protons<sup>3</sup>.

Patients at LBL were treated in the period 1975-1992 with several ions: He, N, O, C, Ne, Si and Ar (REF.<sup>4</sup>). Although most of the patients were treated with light He ions, very heavy ions were also used with the goal of overcoming hypoxia, one of the major causes of cancer radioresistance<sup>5</sup>, which requires charged particles with very high ionization density (linear energy transfer; LET), according to experiments on cells performed at the LBL Bevalac accelerator<sup>6</sup>. However, the entrance channel LET of very heavy ions is relatively high, resulting in unacceptable patient toxicities. Carbon represents a good compromise, with an LET in the entrance channel of  $\sim 12 \text{ keV } \mu\text{m}^{-1}$  and a fairly high LET on the spread-out Bragg peak (SOBP), ranging from 40 to  $80 \text{ keV } \mu\text{m}^{-1}$  (REF.<sup>7</sup>) (FIG. 2). As a result, therapeutic C-ion beams have the advantage of a track structure that is similar to protons in the entrance, but densely ionizing in the tumour, like that of neutrons or  $\alpha$ -particles (see FIG. 2 insets and Supplementary Video 1 for the physical and biological tracks). For this very reason,  $^{12}\text{C}$  ions were chosen for use in cancer therapy first in Japan<sup>8</sup> and then in Europe<sup>9</sup>.

Although heavy ion therapy is the most advanced radiotherapy technology, patient access is problematic, owing to limited capacity. Radiotherapy technology has been continuously upgraded<sup>10</sup>, but not all patients benefit from cutting-edge technologies, including particle therapy or X-ray modern techniques, such as stereotactic body radiotherapy (SBRT)<sup>11</sup>. In the USA, most patients are still treated with conventional 3D conformal radiotherapy, followed by intensity-modulated radiotherapy (IMRT), with only about 1% receiving SBRT or proton therapy<sup>12,13</sup>. In Europe, about a quarter of cancer patients do not receive the radiotherapy they need<sup>14</sup>. As for heavy ion therapy, according to the Particle Therapy Co-Operative Group (PTCOG) database<sup>15</sup>, by the end of 2019, there were eight C-ion centres in Asia and four in Europe that have treated approximately 34,000 patients, with eight more centres under construction or in the planning stage. For comparison, proton therapy is administered at over 100 centres worldwide and has treated over 220,000 patients.

In the US context, the Mayo Clinic in Jacksonville (FL) has advanced plans for building a C-ion therapy facility<sup>16,17</sup>. Its opening would mark a much awaited return of heavy ion therapy in USA after the end of the LBL pilot trial. Until now, concerns about cost-effectiveness and lack of U.S. Food and Drug Administration certification and approved reimbursement have hampered the introduction of C-ion therapy in the USA<sup>18</sup>. The financial

support to treat patients will need to come from federal grants until enough clinical data are available to approach third-party payers in the USA to consider supporting such therapy. Although high investment costs also affect the well-established proton therapy<sup>19</sup>, the cost is even higher for carbon, causing resistance even in the proton therapy community<sup>20</sup>. Yet, some of the clinical results, summarized in this Review, suggest possible improvements in outcomes in some malignancies compared with both X-rays and protons<sup>21,22</sup>. These results have triggered interest in international comparative trials with C ions and investments in preclinical radiobiological research also in the USA, resulting in recent P20 and R01 NCI grants on planning a C-ion facility and heavy ion radiobiology research. In addition, centres with experience in heavy ion therapy such as the National Institutes for Quantum and Radiological Science and Technology (NIRS-QST) in Chiba (Japan) and the Heidelberg Ion Beam Therapy Center (HIT) at the University of Heidelberg in Germany are now testing the use of different ions (especially He (REF.<sup>23</sup>) and O (REF.<sup>24</sup>)) and their combination<sup>25–29</sup> for optimized treatments.

In this Review, we address the question of whether the investment in C-ion therapy is currently justified. Is carbon the ‘silver bullet’ in radiotherapy or should treatments rather use lighter or heavier ions? We first outline the physics and technology of heavy ions, before discussing their radiobiology and surveying relevant clinical results. Finally, we discuss new ions and technologies.

## Physics and technology of heavy ions

All charged particles share the same physics of deposition of energy along their path in matter<sup>30</sup>. The Bragg peak makes particles so appealing compared with X-rays, characterized by a depth-dose curve that decreases exponentially after the initial build-up (FIG. 1). The Bragg peak is the main motivation for charged particle therapy<sup>31</sup>, but there are some notable physical differences as one moves from hydrogen to heavier nuclei<sup>32</sup>.

The energy loss per unit mass length is known as stopping power  $S$  in physics and LET in radiobiology and radiotherapy. It is described by the Bethe-Bloch equation in the framework of the continuous slowing down approximation theory<sup>33</sup>:

$$S = \frac{4\pi N_A e^4}{mc^2} \frac{Z_p^2}{\beta^2} \frac{Z_T}{A_T} \left[ \ln \left( \frac{2mc^2 \beta^2 \gamma^2}{I} \right) - \beta^2 - \frac{C(\beta)}{Z_T} + Z_p L_1(\beta) + Z_p^2 L_2(\beta) + L_3(\beta) \right] \quad (1)$$

where  $e$  is the electronic charge,  $N_A$  the Avogadro number,  $m$  the mass of the electron,  $c$  the speed of light;  $Z_p$  is the effective charge of the projectile,  $\beta$  its relative velocity and  $\gamma$  the Lorentz factor;  $Z_T$  is the atomic number of the target material and  $A_T$  is its mass number. The factor  $I$  in the logarithmic term is the mean excitation energy<sup>34,35</sup>; in human tissues and water, it represents one of the main sources of range uncertainty in particle therapy<sup>36,37</sup>. The additional correction terms are the shell correction  $C$ , Barkas correction  $L_1$ , Bloch term  $L_2$ , and Mott and density corrections  $L_3$ .  $S$  is expressed in  $\text{MeV} \cdot \text{cm}^2 \text{g}^{-1}$  in physics but, in radiobiology and radiotherapy, LET is expressed in  $\text{keV} \mu\text{m}^{-1}$  in water (density  $1 \text{ g cm}^{-3}$ ).

Equation 1 shows that the LET is proportional to the square of the ion charge and, therefore, it can be much higher for heavy ions than for protons, depending on the energy. This is the

key to the biological advantages of heavy ions, because the relative biological effectiveness (RBE) increases with LET, owing to the production of more clustered DNA lesions, which are difficult to repair (Supplementary Video 2). Other differences are related to the nuclear interactions and the scattering, as discussed below.

## Scattering

Beam dispersion in the longitudinal and lateral directions is an important feature in particle therapy. Longitudinal straggling  $\sigma_R$  determines the width of the Bragg peak at a range  $R$ . For two particles of different mass  $M$  at the same range  $R$ , it can be shown that<sup>30</sup>:

$$\frac{\sigma_{R1}}{\sigma_{R2}} = \sqrt{\frac{M_2}{M_1}} \quad (2)$$

Equation 2 shows that longitudinal straggling is lower for heavy ions compared with protons, resulting in a sharper and more precise Bragg peak (FIG. 1).

Lateral scattering for thick targets is dominated by multiple Coulomb scattering and is well described by Molière's theory of multiple scattering<sup>38</sup>. At small scattering angles, Molière's theory approximates the scattering distribution as a Gaussian with standard deviation  $\sigma_\theta$  that can be described as:

$$\sigma_\theta = \frac{14.1 \text{ MeV}}{\beta pc} Z_p \sqrt{\frac{d}{L_{\text{rad}}}} \left[ 1 + \frac{1}{9} \log_{10} \left( \frac{d}{L_{\text{rad}}} \right) \right] \quad (3)$$

where  $d$  is the total mass thickness and  $L_{\text{rad}}$  is the radiation length, which depends on the atomic number  $Z$  of the target material. Equation 3 shows that multiple Coulomb scattering increases for thick and heavy targets (because  $L_{\text{rad}} \approx Z^{-2}$ ), whereas it decreases with particle velocity and, at the same range, with particle mass (FIG. 1). For instance, protons have a lateral scattering that is approximately three times greater than C ions at a depth of 15 cm. However, at greater depths, C-ion projectiles gain substantial contributions to the lateral dose from secondary fragments from nuclear interactions, and the C-ion lateral dose distributions become similar to those of protons<sup>39</sup>.

Lateral scattering is responsible for the dose halo in treatment planning, and makes dose fall-off sharper for heavy ion treatments (FIG. 3). This property is, of course, attractive for sparing organs at risk (OAR), especially in hypofractionation, when the smooth fall-off can produce substantial doses to the OAR surrounding the tumour.

## Fragmentation

Nuclear fragmentation is another major difference between protons and heavy ions. Both produce target fragments (that is, fragmentation of target nuclei, which, in the body, are mostly  $^{16}\text{O}$ ), but protons do not undergo fragmentation after nuclear interactions, whereas heavy ions break into lighter projectile fragments. The nuclear fragmentation cross section  $\sigma_f$  at high energies is well described by the geometric Bradt-Peters approximation<sup>40</sup>:

$$\sigma_f = \pi r_0^2 (A_p^{1/3} + A_T^{1/3} - b)^2 \quad (4)$$

where  $r_0$  is the nucleon radius ( $\sim 1$  fm) and  $b$  the overlapping parameter. Equation 4 shows that the cross section increases  $\sim (A_p)^{2/3}$  and is, therefore, more significant in heavier ions. The projectile fragments have similar velocity and direction to the primary ion but lower charge, and, consequently, have larger range<sup>30</sup>. They generate a ‘dose tail’ beyond the Bragg peak, which is not observed with protons (FIG. 1). The mean free path for 350 MeV/n carbon ions in water (range 20 cm) is approximately 25 cm (REF.<sup>30</sup>), meaning that only about 50% of the accelerated  $^{12}\text{C}$  ions actually reach a deep tumour, the others undergoing nuclear fragmentation. However, in most practical cases, the tail is within the high-dose region in the patient, because two parallel opposed beams are often used for treatment (FIG. 3). Treatments with single beams are indeed generally avoided because of the problem of the range uncertainty, which is the main physics problem limiting the precision of particle therapy and which also affects proton therapy<sup>41</sup>.

At the same time, fragmentation can be beneficial for treatment monitoring and reducing range uncertainty. Image guidance is indeed essential for heavy ions, even more so than for X-rays. In fact, the sharp dose gradients in heavy ion therapy become a problem if the target is missed and the Bragg peak occurs in an OAR. In clinical particle therapy, a substantial margin is added to the prescribed range in order to ensure tumour coverage. For instance, in proton therapy, this range margin is on the order of 3.5% of the prescribed range<sup>42</sup>. Wide margins jeopardize one of the main advantages of the Bragg peak: the steep dose gradients and the potential high accuracy and precision<sup>43</sup>. It is, therefore, desirable to monitor heavy ion treatments precisely and, thereby, reduce these margins.

Unfortunately, image guidance was originally developed for X-rays and is taking time to be fully exploited in particle therapy, where additional complications can occur, for instance, in using magnetic resonance imaging online guidance. However, the physics of charged particles offers unique opportunities for in vivo range verification<sup>30,44</sup>. The range verification method that has been tested most extensively in clinical practice is positron emission tomography (PET)<sup>45</sup>. In C-ion therapy, fragmentation of the primary ion generates positron-emitting isotopes, especially  $^{11}\text{C}$ . Positron annihilation with electrons produce two 511-keV  $\gamma$ -rays emitted at  $180^\circ$  to each other that can be visualized by PET. An online PET, that is, a PET system that is positioned around the patient and works during the treatment, was used at GSI for treatment monitoring and range verification<sup>46</sup>, and offline PET imaging (that is, imaging of the patient with a PET in a different room following the treatment) is currently in use in other C-ion centres<sup>47</sup>. A similar approach can be used with heavier ions. For example,  $^{16}\text{O}$  produces positron-emitting  $^{15}\text{O}$ , which can be visualized by PET. In proton therapy, only target fragments can be used for imaging, whereas in heavy ion therapy, the projectile fragments provide a large part of the signal.

However, the activity peak invariably occurs upstream of the Bragg (dose) peak, because the light fragments have shorter range at the same velocity of the primary ion<sup>30</sup>. The peak shift, along with biological washout and the efficiency of the detectors systems, makes resorting to Monte Carlo simulations in data analysis currently unavoidable. All these corrections

currently limit the accuracy of PET-based range verification to about 2-5 mm (REF<sup>44</sup>). The problem could be solved by using radioactive ion beams directly for treatment. Radioactive ion beams would improve the count rate by an order of magnitude<sup>48</sup>, reduce the shift between measured activity and dose, and mitigate the washout blur of the image with short-lived isotopes and in-beam acquisition, eventually leading to sub-millimetre resolutions. However, attempts to use these beams in therapy have been hampered by the low intensity of the secondary beams produced by fragmentation of the primary, stable ion<sup>49</sup>. With modern, high-intensity accelerators, it is possible to produce radioactive ion beams with an intensity sufficient for therapeutic treatment<sup>50</sup>, and such beams would pave the way to PET-guided heavy ion treatment. Several studies are ongoing to assess the advantages of radioactive ion beams for therapy<sup>51</sup>, and a prototype for a compact PET cyclotron producing <sup>11</sup>C beams as an injector for a medical synchrotron has been proposed by CERN<sup>52</sup>.

## Accelerators

In the past, orthovoltage X-ray tubes and <sup>60</sup>Co  $\gamma$ -rays sources were used for cancer therapy, but, today, all radiotherapy is based on electron or hadron accelerators<sup>53</sup>. Compact linear accelerators (linacs) are used to accelerate electrons to 6-25 MeV. The electrons then produce high-energy X-rays by bremsstrahlung in a metallic target. Although there are many research projects on the use of linacs for particle therapy<sup>54</sup>, at present, all particle therapy facilities use circular accelerators, either cyclotrons or synchrotrons<sup>30</sup>, in which particles are bent by a magnetic field  $\mathbf{B}$  and accelerated by an electric field. The gyroradius  $\rho$  in a particle accelerator is determined by the magnetic rigidity (expressed in Tm):

$$B\rho = \frac{p}{q} \quad (5)$$

where  $p$  is the momentum of the particle and  $q$  is its charge. According to Eq. 5, a synchrotron accelerating 400 MeV/n <sup>12</sup>C ions must have a diameter approximately three times larger than a 250-MeV proton synchrotron for equal  $B$  field. Most proton therapy centres are based on cyclotrons, but for heavier ions, a cyclotron would be very massive and, currently, all C-ion centres use large synchrotrons. The comparison in FIG. 4a shows the impact of magnetic rigidity on the footprint and complexity of the machine, resulting in increasing cost.

Currently, there are many efforts to reduce the footprint and cost of accelerators. These efforts are mostly directed towards the use of superconducting magnets<sup>55</sup> that increase the strength  $B$  of the magnetic field (from approximately 1.8 T in resistive magnets up to 4–9 T for superconductive magnets), thus, allowing a reduction of the radius at the same rigidity (Eq. 5). Superconducting cyclotrons are already in use for proton therapy (such as IBA S2C2 and Varian ProBeam), and several projects for heavy ion superconducting cyclotrons<sup>56</sup> or synchrotrons<sup>57,58</sup> (FIG. 4b) are ongoing. Superconducting magnets in medical accelerators pose several problems. To achieve high fields ( $B > 3$  T), a large quantity of superconducting material is needed, resulting in high cost and challenging cooling. Magnets in synchrotrons need field ramp rates  $>1$  T s<sup>-1</sup>, a curved shape and, usually, quadrupole integration. The options are Nb–Ti (Nb<sub>3</sub>Sn)<sup>59</sup>, cosine theta or canted cosine theta<sup>60</sup> and high-temperature superconductors<sup>61</sup>. Nb–Ti is predominant because of its good industrial development and



higher reliability, while Nb<sub>3</sub>Sn is used only for applications where the very high fields cannot be avoided.

All these options are currently under testing for applications in medical accelerators and gantries. FIGURE 4c shows the concept of a compact medical synchrotron using alternating gradient canted cosine theta superconducting magnets developed at CERN. The circumference is approximately 30 m, whereas the present-day third-generation Japanese models (FIG. 4b) are longer than 60 m.

This R&D is likely to lead to substantially smaller — and cheaper — heavy ion machines in the next 10 years.

Larger uncertainties are associated to the development of new, potentially revolutionary accelerator technologies, such as dielectric wall accelerators<sup>62</sup> and laser-driven particle accelerators<sup>63–65</sup>. Many research groups have worked on laser-accelerated particles over the past 20 years but, despite many recent efforts for designing beam transport and delivery in therapeutic scenarios<sup>66,67</sup>, problems remain, including<sup>68</sup>: increasing the intensity; increasing the maximum particle energy; shielding for secondary radiation (especially the very abundant low-energy ions), which is likely to be bulky and expensive; target stability; improving shot-to-shot reproducibility (at least to the few % level); and addressing quality assurance and patient safety aspects. Full laser-driven ion medical accelerators remain far in the future, but low-energy linear injectors in ring accelerators could be laser-driven. The current plans for miniaturized synchrotrons in Japan (fifth model in FIG. 4b) include the use of a short laser-driven particle accelerator as injector for a high-*B*-field superconducting synchrotron<sup>69</sup>.

## Beam delivery

New proton therapy centres all deliver the beam using pencil beam scanning (PBS), in which the whole tumour volume is scanned in 3D using a narrow pencil beam<sup>30</sup> (Supplementary Video 3). PBS is also used in the majority of C-ion centres, with only a few centres in Japan still using the old passive modulation systems. PBS provides an unsurpassed conformity, but is problematic for moving targets, especially thoracic and abdominal tumours that move with breathing. The problem is caused by the interplay between beam and tumour movements, resulting in poor dose distributions. The problem is tackled with different motion mitigation techniques<sup>70–72</sup>, but some simple methods such as gating leave the problem of the residual motion, whereas accurate 3D tumour tracking with the beam requires complex online fast movement and range adaptation. A simpler way to handle range changes and complex motion patterns is 4D treatment planning, in which the plan is optimized from a full 4D computed tomography (CT) scan of the tumour, thus, including the motion. This technique is ideal for particle therapy<sup>73</sup>, and, in particular, for therapy with heavy ions<sup>74</sup>, in which the interplay between beam scanning and target motion produces poor target coverage.

An optimal dose distribution always requires irradiation from different angles, and even the Bragg peak means that the number of beams is reduced in particle therapy. In linacs, the beam is bent by a magnet that can rotate around the patient (gantry) to irradiate from different angles or even continuously rotate around the patient (tomotherapy or volumetric

modulated arc therapy). Gantries for protons are bigger and separated from the accelerator, with the exception of the Mevion S250 system, in which the cyclotron itself is mounted on a gantry. Gantries for heavy ions are larger and heavier than proton gantries, again to match the increased magnetic rigidity (Eq. 5). The HIT gantry, with resistive magnets, is a 670-tonne structure with diameter of 13 m. It was the first gantry for heavy ions and has been in clinical operation for a decade. As discussed above in the context of synchrotrons, smaller and lighter gantries should use superconducting technology<sup>60,61,69</sup>. A lighter (300 tonne) superconducting gantry has been installed in the new PBS treatment facility at NIRS<sup>75</sup>.

Even using modern superconducting magnets, the gantry remains one of the most expensive and bulky items in heavy ion therapy. Certainly an easy way to reduce the cost of a heavy ion facility would be to use only fixed lines, including vertical, horizontal and oblique lines, as is done in several C-ion centres in Europe and Asia. However, this setup limits the angles that can be used, effectively penalizing heavy ion therapy in comparison with IMRT or proton therapy, in which gantries are always provided.

As an alternative to moving the beam, it could be possible to move the patients using a dedicated chair. Irradiation with neutrons and charged particles of patients immobilized on a treatment chair was in use already in the 1950s<sup>76</sup>, and is still the standard for treating ocular tumours with protons. The method was abandoned for targets outside the skull because the patient must still lie down for the planning CT, and, therefore, the recorded organ positions are different to those when the patient is sitting. However, the situation changed with the introduction of vertical CT, which provides images for planning that are obtained with the patient in the same vertical position as the treatment. The irradiation in upright position of thoracic tumours has the potential additional advantage of reduced respiratory motion<sup>77</sup>. The Northwestern Medicine Center in Chicago, USA, is currently treating patients in an upright position with protons, following treatment plans from vertical CT. Optimal flexibility in gantry-less systems can be achieved using chairs with six degrees of freedom, that is, using a 360° rotating platform, an XYZ translation and enabling the chair to tilt. A six-degrees-of-freedom chair has been installed at the Shanghai Proton and Heavy Ion Center (SPHIC) C-ion centre in Shanghai, China, for the treatment of head and neck tumours<sup>78,79</sup>.

## Radiobiology

Beyond the physical differences between heavy ions and protons and photons, the real motivation for using heavy ions lies in biology. In fact, as discussed above, heavy ions have higher LET than photons and protons, resulting in more powerful radiobiological effects caused by the different DNA lesion patterns and quality at the micrometre and nanometre scales<sup>80</sup> (Supplementary Videos 1 and 2). As shown in FIG. 2, carbon ions have low LET in the entrance channel and high LET in the SOBP. Therefore, their radiobiological properties are similar to protons and X-rays in normal tissue, but similar to neutrons and  $\alpha$ -particles in the tumour. Fast neutrons<sup>81</sup> and  $\alpha$ -particles<sup>82</sup> are both used in cancer treatment, but they have caveats compared with heavy ions: for neutrons, the depth-dose distribution is similar to X-rays and the LET is constant along the beam path; short-range  $\alpha$ -particles can only be used for internal exposure in the framework of targeted radioimmunotherapy.



The radiobiological features of heavy charged particles have been recently reviewed<sup>7,83,84</sup> and are summarized in FIG. 5. The survival curves in FIG. 5 are generally described by the linear–quadratic (LQ) model<sup>85</sup>:

$$S = e^{-\alpha D - \beta D^2} \quad (6)$$

where  $S$  is the surviving fraction to a dose  $D$  of radiation. The cell radiosensitivity is determined by the fitting parameters  $\alpha$  and  $\beta$ , usually using their ratio. The LQ model is a consequence of Poisson statistics and the quadratic term corresponds to inter-track lethal events, which are more likely for sparsely ionizing radiation than for heavy ions. At high LET,  $\alpha$  tends to increase and  $\beta$  tends to decrease<sup>86</sup>, resulting in survival curves that are almost exponential. The ratio  $D_X/D_p$  of the doses of the reference radiation X (X-rays) and particle radiation p producing the same survival is the RBE for cell killing, which Eq. 6 shows is higher at low doses than at high doses, especially when the  $\alpha/\beta$  ratio is low. Even if the LQ model is only applicable in the low-dose range, typical of conventional fractionation in radiotherapy, it can be extended to high dose per fraction, such as procedures used in SBRT<sup>87</sup>.

The preclinical studies at LBL<sup>6</sup> had already demonstrated that, in addition to the increased RBE for cell killing, heavy ions have reduced oxygen enhancement ratio (OER), reduced dependence from the cell cycle phase and reduced dependence on dose rate or fractionation. More modern observations have shown reduced angiogenesis<sup>88,89</sup>, as well as synergistic effects in combination with targeted therapy<sup>90</sup> and immunotherapy<sup>91</sup>.

## RBE

Certainly the increased RBE for cell killing is the best known advantage of heavy ion therapy. The RBE increases with LET up to a maximum around 100–200 keV  $\mu\text{m}^{-1}$  (REF.<sup>86</sup>), whereas it decreases again at very high LET (a phenomenon known as the overkilling effect)<sup>92</sup>. The RBE increases the SOBP peak/plateau ratio in heavy ion therapy compared with proton therapy, because it is higher in the target region (peak; high LET) than in the normal tissue (entrance; low LET). The dose in the target region in heavy ion therapy is usually optimized using a RBE-weighted dose defined by the International Commission on Radiological Units (ICRU) as<sup>93</sup>

$$D_{\text{RBE}} = \text{RBE}(E, D, a, b, c) \cdot D(\text{Gy}) \quad (7)$$

where the physical dose in gray (1 Gy = 1 J  $\text{kg}^{-1}$ ) is corrected by the dimensionless RBE factor, which is a function of the dose, the particle energy  $E$  and several other factors ( $a$ ,  $b$ ,  $c$ ...), such as dose rate, oxygen concentration, intrinsic radiosensitivity, among others. Given its dependence on so many parameters, the RBE can only be calculated by a biophysical model such as the micro-dosimetric kinetic model<sup>94</sup> or the local effect model<sup>95</sup>, both based on the LQ model (Eq. 6).

At present, the uncertainty on C-ion RBE models is perceived as a major problem in heavy ion therapy compared with proton therapy<sup>3</sup>. Although it is generally acknowledged that the proton RBE is also variable<sup>96</sup>, the variation is considered small enough to allow the use of a

simple constant RBE = 1.1 along the whole SOBP<sup>97</sup>. (However, the situation may change in the future, and, in some centres, RBE models are now used in proton therapy<sup>98</sup>.) For carbon, the RBE-weighted dose calculated by different models for the same physical C-ion dose can differ substantially<sup>99,100</sup>, and, for this reason, great care has to be taken in comparing the clinical results from different heavy ion centres, even if the same RBE-weighted dose is reported<sup>101,102</sup>.

Among the various parameters, notable for radiotherapy is the RBE dependence on the intrinsic radiosensitivity (that is, the  $\alpha/\beta$  ratio, derived from the X-ray dose-response curve; Eq. 6) and on the dose per fraction. The RBE decreases when the intrinsic radiosensitivity of the tissue or the dose per fraction are increased. Accordingly, the maximum RBE advantage is observed for radioresistant tumours (FIG. 6). The fractionation dependence is intertwined with the radiosensitivity, because the RBE decrease at high doses is faster for radioresistant than for radiosensitive tissues, that is, the RBE in hypofractionation decreases<sup>103,104</sup> more sensitively for normal tissue ( $\alpha/\beta \approx 2$  Gy) than for the tumour ( $\alpha/\beta \approx 10$  Gy)<sup>105</sup>. Therefore, even if the RBE is low at high dose per fraction, hypofractionation is possible and, indeed, is often pursued in clinical treatments with heavy ions<sup>106</sup>.

## Hypoxia

Most tumours are hypoxic, which increases their resistance to treatments with either conventional drugs or radiation<sup>107</sup>. Fractionation in radiotherapy is used to overcome hypoxia, by exploiting interfractional reoxygenation. This advantage is, however, lost in the modern hypofractionated regimes, making hypoxia a major problem for SBRT<sup>108,109</sup>. The OER — that is, the ratio of the doses producing the same effect in hypoxic (0% pO<sub>2</sub>) and oxic (20% pO<sub>2</sub>) conditions — is approximately 3 for X-rays, a value so high that, if translated to the clinic, would make radiotherapy of hypoxic tumours impossible without reoxygenation. In reality, physiological hypoxia is, on average, only 5% in normal tissue and <2% in most tumours<sup>110</sup>. The OER decreases at high LET<sup>111</sup>, because, for densely ionizing particles, the damage is induced by direct effects on the DNA molecule and free radicals play a smaller role than they do for X-ray-induced damage. In cellular studies, it is known that the OER drops to 1 at LET  $\approx 200$  keV  $\mu\text{m}^{-1}$  at physioxic concentrations<sup>112</sup>. However, this result indicates that the LET for C ions (FIG. 2) is not high enough to overcome hypoxia in the tumour. Thus, interest in heavier ions and multi-ion treatments is justified, as discussed in the next section.

## Combined treatments

Radiotherapy is often used in combination with drug treatments, including chemotherapy, targeted therapy and immunotherapy<sup>113</sup>. Can heavy ions be more effective than X-rays in combined treatments? Some preclinical studies of the combination of carbon ions with targeted therapies suggest a synergistic effect<sup>90</sup>. The synergism depends on the mechanisms of radiation damage, and, therefore, different drugs can be used for X-rays and heavy ions. However, for immunotherapy, heavy ions have a physical advantage, because they spare much better the patients' own immune cells, owing to the reduced integral dose compared with other treatments<sup>114</sup>. This putative advantage is shared with proton therapy<sup>91,115</sup>, for which reduced lymphopaenia has been observed compared with X-ray treatment for

oesophageal cancer<sup>116</sup>, glioblastoma<sup>117</sup> and lung cancer<sup>118</sup>. Preclinical data in a mouse osteosarcoma model also shows that high C-ion doses have biological advantages compared with X-rays in combination with immune checkpoint inhibitors<sup>119,120</sup>. Specific trials to address the combination of heavy ions and immunotherapy are highly desirable and may prove a breakthrough in combined treatment protocols using immunotherapy<sup>121</sup>. Modelling the combination with biophysical models is necessary to achieve an optimal combination<sup>122</sup>.

## Clinical results

The clinical data obtained with carbon ions are reviewed in many recent publications<sup>8,16,21,22,83</sup>, and, therefore, we only briefly describe below the most promising tumour sites in which differences are expected not only with respect to X-rays but also to proton therapy. We focus on the sites in which carbon ions gave the best results, pending ongoing clinical trials.

### Eye tumours

Uveal melanoma is one of the most common diseases treated with proton therapy, but heavier ions have also been used<sup>123</sup>. Interestingly, the only phase III comparative clinical trial completed for ions heavier than protons is for choroidal and ciliary body melanoma of the eye. The trial compared accelerated He ions to <sup>125</sup>I plaque therapy for patients treated in the LBL trial. The results of long-term outcomes of 184 patients treated during the period 1985–1991 were published in 2015 (REF.<sup>124</sup>) and show significantly improved local control, eye preservation and disease-free survival. Even if this is a limited trial for a rare tumour, it shows that well-designed trials with long outcome can give significant results.

### Gastrointestinal cancers

In an independent review of 20 years of C-ion therapy at NIRS-QST in Japan<sup>125</sup>, the panel noted that the most striking and remarkable outcomes had been observed for gastrointestinal tumours, such as pancreas and local recurrence of rectal cancer.

The results obtained at NIRS-QST for locally advanced pancreatic adenocarcinoma treated with hypofractionated C ions with concurrent gemcitabine<sup>126</sup> were confirmed in a multi-institutional Japanese trial<sup>127</sup>. These results have attracted great interest, because pancreatic cancer is difficult to detect early and is so resistant to treatment that it is becoming a leading cause of cancer death<sup>128</sup>. Considering that pancreatic cancers are very hypoxic<sup>129</sup> and their microenvironment is markedly immunosuppressive<sup>130</sup>, it has been hypothesized that C ions, with their low OER and increased immunogenic cell death, can be the ‘silver bullet’ for this highly lethal malignancy<sup>131</sup>. As a result, pancreatic cancer is considered one of the most interesting comparative clinical trials to be pursued with C ions<sup>132,133</sup>.

Also exceptional are the outcomes of C-ion treatment for another tumour with high lethality, namely, locally recurrent rectal cancer. In a multi-centre Japanese clinical trial, survival rates with concomitant chemotherapy in the high-dose C-ion group was 90% at 2 years and 50% at 5 years<sup>134</sup>. Similar results were confirmed in a trial with similar doses at the SPHC<sup>135</sup>, and good preliminary results were also obtained at the HIT<sup>136</sup>. These clinical data indicate

a clear improvement compared with the best results of chemoradiotherapy using IMRT<sup>137</sup>, and are similar to the outcome of surgical resection for this malignancy<sup>138</sup>.

Excellent results have also been reported for hepatocellular carcinoma, especially large tumours close to the porta hepatis<sup>139</sup>. Both carbon ions and protons present lower toxicity than SBRT or 3D conformal radiotherapy<sup>140</sup>, but carbon ions are delivered in shorter treatments of about four fractions<sup>141</sup> up to a RBE-weighted dose of approximately 60 Gy (REF.<sup>142</sup>).

## Sarcomas

Sarcomas are traditionally considered radioresistant cancers, and, therefore, excellent candidates for heavy ion therapy<sup>143</sup>. The poor radiation response of sarcomas compared with other cancers, such as carcinomas, does not seem to be linked to genetic radiosensitivity but, rather, to slow growth of the tumours and the presence of hypoxia, especially in large, unresectable malignancies<sup>144</sup>. Most particle therapy centres treat sarcomas, especially chordomas and chondrosarcomas of the base of the skull<sup>145</sup>.

The Japanese results with C ions for osteosarcomas of the trunk<sup>146</sup> and soft tissue sarcomas<sup>147</sup> are excellent, especially for inoperable large tumours that are difficult to treat. First results from the Centro Nazionale di Adroterapia Oncologica (CNAO) in Italy also support these results<sup>148</sup>. At the HIT, a prospective phase I/II trial with a combined proton and C-ion radiotherapy has been completed, showing favourable toxicity and high response rates<sup>149</sup>.

The HIT in Heidelberg has made a long-term follow-up of 155 skull base chordoma patients treated in the C-ion pilot project at GSI in Darmstadt over the period 1998–2008 and the results are excellent, with an overall survival of 75% at 10 years<sup>150</sup>. Excellent results are also reported for skull base chondrosarcoma, but no significant differences between protons and carbon ions were observed in terms of local control or overall survival in 101 patients, with a median follow-up of 40 months from the treatment at the HIT over the period 2009–2014 (REF.<sup>151</sup>). The hypothesis of the study is that carbon ion radiotherapy can achieve the same local control at lower toxicity than other treatments. The results of the phase III trial are preliminary<sup>152</sup> and more time is needed to draw final conclusions, but early results suggest that a favourable physical dose distribution is the main factor to reduce toxicity and achieve local control in chondrosarcoma.

## Head and neck tumours

Cancers located in the upper aerodigestive tract are often candidates for particle therapy, because they are surrounded by OAR and patients experience severe toxicities from treatments<sup>153</sup>. The rationale for using heavy particles rather than protons is both a reduced dose halo (FIG. 3) and the biological advantages (FIG. 5). Physics advantages can be exploited to provide a boost at the end of IMRT treatments<sup>154</sup>, and the biological advantages can be used for radioresistant histologies<sup>155</sup>. C-ion therapy is typically indicated for salivary gland tumours such as adenoid cystic carcinoma<sup>156</sup> and nasopharyngeal carcinoma<sup>157</sup>, with randomized clinical trials under way for these pathologies. Comparative trials are important to assess whether heavy ions can do better than protons, which have already

demonstrated a significant mitigation of toxicity compared with IMRT in combination with chemotherapy<sup>158,159</sup>.

### Paediatric tumours

Paediatric cancers are typical candidates for proton therapy, considering that sparing normal tissue, often the brain, is particularly important for patients with long life expectancy<sup>160</sup>. Approximately 10% of paediatric solid tumour patients in the USA were treated with protons in 2012 (REF.<sup>13</sup>), and this fraction is growing rapidly.

Heavy ions have been traditionally deemed too risky for paediatric patients. In fact, high-LET radiation has high RBE for late effects, including carcinogenesis<sup>161</sup>. The concern for possible induction of second cancers has, therefore, limited the use of high-LET heavy ions in paediatric patients. However, in a cohort of 83 patients aged <21 years treated at the HIT, no significant differences were observed in normal tissue toxicity after treatment with protons or C ions<sup>162</sup>. Moreover, the concern for second cancers after high-LET radiation has been contradicted, at least for adult patients, by a retrospective analysis of 1,580 prostate cancer patients treated with C ions at NIRS<sup>163</sup>. The study found a lower risk of second cancers in patients treated with heavy ions compared with those treated with X-ray therapy. This outcome is also consistent with measurements of secondary radiation, including neutrons, in PBS therapy<sup>161</sup>, and, therefore, it has been proposed that C ions may be an excellent tool in paediatric patients<sup>164</sup>.

In addition, helium ions are potentially ideal for children, because they have low RBE, similar to protons (FIG. 2), but sharper dose distributions, thus, providing increased sparing of normal tissue (FIG. 3). An *in silico* study in different paediatric pathologies has shown advantages of He ions for neuroblastoma, Wilms tumours and ependymoma<sup>165</sup>.

### New ions and technologies

At present, particle therapy is limited to protons and C ions, but several other ions could be used to treat solid cancers. Carbon ions exhibit a good compromise between low LET in the normal tissue and high LET in the target region (FIG. 2). However, for radiosensitive tumours, light ions can have better properties than heavy ions (FIG. 6), and, even for radioresistant tumours, He ions can be as good as carbon in normoxia.

### Helium ions

In a pilot project at LBL, over 2,000 patients were treated with <sup>4</sup>He ions<sup>4</sup>. Helium should be selected when one is not faced by a tumour that is particularly radioresistant and/or hypoxic, but one does want an increased precision and reduced dose 'halo' (FIG. 3), achieved thanks to the reduced lateral scattering. Acceleration of <sup>4</sup>He is complicated by beam contamination with heavier ions with the same  $q/m$  ratio from the ion source, which have the same rigidity as helium and are, therefore, accelerated by the synchrotron. For this reason, it has been proposed to use <sup>3</sup>He for therapy<sup>166</sup>, which has similar properties to <sup>4</sup>He but with limited contamination problems, and would result in smaller and cheaper He-dedicated accelerators, thanks to the lower rigidity of <sup>3</sup>He (Eq. 6). A calculation with two opposite fields using the local effect model (FIG. 6) suggests that, for both a radiosensitive ( $\alpha/\beta = 10$  Gy) or

a radioresistant ( $\alpha/\beta = 2$  Gy) tumour, helium gives a lower dose to the normal tissue for the same target dose<sup>167</sup>. These simulations show that helium can be very useful in different scenarios. The HIT will start using helium ions in clinical treatments in 2022, following extensive preclinical studies<sup>23,27</sup>.

### Oxygen ions

Ions heavier than carbon can be interesting for very radioresistant, hypoxic tumours. In simulations of normoxic tumours, ions heavier than carbon do not seem to have advantages (FIG. 6). However, for hypoxic cancers,  $^{16}\text{O}$  ions are expected to be more effective than  $^{12}\text{C}$  ions<sup>168,169</sup>. As noted in the introduction, overcoming hypoxia was the main motivation to use very heavy ions in the LBL trial, but very heavy ions such as  $^{40}\text{Ar}$  have a high LET, even in the entrance channel, leading to unacceptable toxicities. In the entrance channel, oxygen is still in the low-LET region (FIG. 2), and, therefore, relatively safe. For this reason, the HIT is planning to use oxygen ions for treatment of very hypoxic tumours<sup>24,27</sup>.

### Multi-ion treatment

Even when using ions heavier than carbon, it remains difficult to deliver a high-LET treatment to the whole tumour volume (FIG. 2); only a relatively small fraction of the tumour is exposed to high LET. The optimization on the biological dose can, therefore, jeopardize the putative biological advantages (FIG. 5) of heavy ion therapy<sup>7</sup>. The problem is now emerging also in the clinics. A retrospective analysis on the C-ion treatment plans at NIRS suggest that the LET is positively associated to local control of pancreas tumours. In particular, patients with higher minimum dose-averaged LET values in the gross tumour volume had lower probability of local failure compared with those with minimum LET values below  $40 \text{ keV } \mu\text{m}^{-1}$  (REF.<sup>170</sup>). Similar results have been observed looking at local recurrence maps in grade 2 chondrosarcoma patients treated at NIRS with C ions<sup>171</sup>.

Approaches to extend the high-LET regions with a single ion (LET painting<sup>172,173</sup>) are hampered by increasing toxicity. However, when multiple ions (light to heavy) are used, it is possible to increase the LET in the target region while maintaining a low toxicity in the normal tissue<sup>174</sup>. A combination of protons, helium, carbon and oxygen beams, produced at the same synchrotron, can be delivered to achieve a prescribed LET map to the target, in a method known as intensity-modulated composite particle therapy. For instance, in a simulated prostate treatment aiming to deliver 2 Gy to the planning target volume, it is possible to have  $80 \text{ keV } \mu\text{m}^{-1}$  in the gross tumour volume,  $50 \text{ keV } \mu\text{m}^{-1}$  in the clinical target volume and  $<30 \text{ keV } \mu\text{m}^{-1}$  in the OAR (rectum)<sup>175</sup>. This method requires a multi-ion source synchrotron, like those available at the HIT<sup>25</sup> or NIRS<sup>26,28</sup>. In addition, it will be necessary to implement a careful multi-angle dose simulation and verification and fast switching among different ion sources. For applications to hypoxic tumours, multi-ion optimization requires quantitative hypoxia imaging using molecular imaging methods<sup>176</sup>. If an  $\text{O}_2$  concentration map is available, multi-ion treatments can optimally increase the LET (decreasing the OER) or the dose in the low-oxygen sub-volumes, resulting in highly effective treatments for hypoxic tumours<sup>29</sup> (FIG. 7). Multi-ion therapy, therefore, has a number of technical challenges, but the goal of increasing the LET in the tumour volume is an important step towards the optimization of heavy ion therapy.



## New beam delivery methods

We have already noted that the use of very heavy ions, although advantageous for hypoxic tumours, is hampered by normal tissue toxicity. One would, therefore, like a technique that spares normal tissue much more than existing methods do. In this regard, two hot topics in radiotherapy at present are FLASH and spatially fractionated radiotherapy<sup>177</sup>.

FLASH radiotherapy is a method to deliver the therapeutic dose at very high dose rate ( $>40 \text{ Gy s}^{-1}$ ). At ultra-high dose rates, there is a substantial sparing of the normal tissue while maintaining local tumour control<sup>178–180</sup>. These extremely high dose rates are difficult to reach with the high-energy X-rays used in radiotherapy, because of the small conversion efficiency of the bremsstrahlung production process. However, the dose rates have been achieved with charged particles, including electrons<sup>181</sup> and protons<sup>182</sup>, and can also be attained at synchrotrons with heavier ions<sup>183</sup>. It also seems that sparing the normal tissue by FLASH depends not only on the dose rate but on many other parameters, including also total dose, time structure of the beam and tissue oxygenation. The best conditions seem to be achieved around 10 Gy total dose delivered in  $<100 \text{ ms}$  at dose rates  $>10 \text{ Gy s}^{-1}$  in slightly hypoxic tissues<sup>184,185</sup>. The topic is alluring for accelerator physicists, who have already produced a number of ideas and prototypes for FLASH-dedicated machines. The laser-driven accelerators (discussed in the section on accelerators) would be ideal for FLASH radiotherapy, given their very high dose per pulse<sup>186</sup>. However, it should be pointed out that the clinical applications have barely started<sup>187</sup>, and that the mechanism of the FLASH effect is still unclear. Several models have been proposed based on radiation chemistry mechanisms, such as oxygen depletion<sup>188</sup> or free radical recombination<sup>189</sup>, but none has been supported experimentally<sup>190</sup> and the models often also have theoretical flaws<sup>191</sup>. In the absence of a solid theoretical interpretation, it is unknown whether the FLASH effect will be observed for high-LET radiation. This question is currently under investigation<sup>192</sup>.

Another delivery technique that substantially spares normal tissue is spatially fractionated radiotherapy, in which the therapeutic beam is divided into beam-lets spaced by a few micrometres (microbeam radiotherapy)<sup>193</sup> or millimetres (minibeam radiotherapy)<sup>194</sup>. This grid configuration greatly improves the repopulation capacity of the normal tissue<sup>195</sup>, and the target tumour can be covered with interlaced beams<sup>196</sup>. The method has been used in a rabbit with C ions<sup>197</sup> and can be extended to heavier ions<sup>198,199</sup>, exploiting the spatial fractionation to reduce toxicity.

FLASH and minibeam radiotherapy are approaching clinical utilization, but they have the potential to become useful tools in heavy ion therapy<sup>200</sup>. These methods widen the therapeutic window that is appealing even for protons, but may allow the use of ions heavier than oxygen against very radioresistant tumours, making possible one of the ideas that sparked their initial development<sup>2</sup>.

## Outlook

The quest for a ‘cure-all’ particle in radiotherapy will never find a simple solution. Cancers have proven to be very different to each other and elusive to the most advanced therapies,

and, certainly, there is not a magic particle able to destroy all types of malignancies. Based on the present state of the art, we argue that heavy ion therapy is at a tipping point: it has an enormous potential thanks to favourable physical (FIG. 1) and biological (FIG. 5) properties, but its clinical advantage compared with protons and X-rays — which are both cheaper and smaller technologies (FIG. 4) — remains unproven. Some outstanding results have been obtained in gastrointestinal cancers (especially in the pancreas), sarcomas and nasopharyngeal carcinomas, but randomized clinical trials are ongoing. The plans for new centres in Europe, Asia and the USA are, therefore, welcome, if those centres will be used for clinical research and comparative trials.

At the same time, research must continue to make the therapy cheaper and more effective. In physics, it is particularly important to build smaller and cheaper accelerators and beam delivery systems, exploiting superconducting magnets and gantry-less systems. In biology, it is essential to assess the combination of heavy ions with molecular therapy and immunotherapy, in comparison with X-rays and protons. In clinical research, it is necessary to test hypofractionated regimes, combined protocols and to fully exploit the putative advantages listed in FIG. 5 by increasing the LET in the tumour. In fact, the relatively modest LET values reached in large fractions of the cancer volume treated with C ions (FIG. 2) raises the question of whether the main biological advantages of densely ionizing radiation is being squandered. Higher LET in the target volume can require multi-ion irradiation (FIG. 7), and, therefore, rather than a single silver bullet, in the future, a combination of projectiles may become common to sterilize aggressive, radioresistant malignancies.

## Supplementary Material

Refer to Web version on PubMed Central for supplementary material.

## Acknowledgements

The authors thank Uli Weber, Emanuele Scifoni, Olga Sokol, Daria Boscolo, Burkhard Jakob, Anastasiia Quarz, Koji Noda and Elena Benedetto for their precious assistance in the preparation of the figures. The research activities at GSI and Heidelberg Ion Beam Therapy Center (HIT) are partly supported by the EU Horizon 2020 research and innovation programme under grant agreement no. 101008548 (HITRI*plus*). Projects on innovative beam delivery at GSI are supported by ERC advanced grant 2020 number 883425 (BARB).

## References

1. Wilson RR. Radiological use of fast protons. *Radiology*. 1946; 47 :487–491. [PubMed: 20274616]
2. Tobias CA. Failla Memorial lecture. The future of heavy-ion science in biology and medicine. *Radiat Res*. 1985; 103 :1–33. [PubMed: 3906741]
3. Durante M, Loeffler JS. Charged particles in radiation oncology. *Nat Rev Clin Oncol*. 2010; 7 :37–43. [PubMed: 19949433]
4. Castro JR. Results of heavy ion radiotherapy. *Radiat Environ Biophys*. 1995; 34 :45–48. [PubMed: 7604160]
5. Colliez F, Gallez B, Jordan BF. Assessing tumor oxygenation for predicting outcome in radiation oncology: a review of studies correlating tumor hypoxic status and outcome in the preclinical and clinical settings. *Front Oncol*. 2017; 7 :10. [PubMed: 28180110]
6. Blakely EA, Ngo F, Curtis S, Tobias CA. Heavy-ion radiobiology: cellular studies. *Adv Radiat Biol*. 1984; 11 :295–389.

7. Tinganelli W, Durante M. Carbon ion radiobiology. *Cancers*. 2020; 12 :3022.
8. Tsujii, H, , et al. Carbon-Ion Radiotherapy. Springer; 2014.
9. Kraft G. Tumor therapy with heavy charged particles. *Prog Part Nucl Phys*. 2000; 45 :473–544.
10. Thariat J, Hannoun-Levi J-M, Sun Myint A, Vuong T, Gérard JP. Past, present, and future of radiotherapy for the benefit of patients. *Nat Rev Clin Oncol*. 2012; 10 :52–60. [PubMed: 23183635]
11. Lo SS, et al. Stereotactic body radiation therapy: a novel treatment modality. *Nat Rev Clin Oncol*. 2010; 7 :44–54. [PubMed: 19997074]
12. Pan HY, Jiang J, Shih YCT, Smith BD. Adoption of radiation technology among privately insured nonelderly patients with cancer in the United States, 2008 to 2014: a claims-based analysis. *J Am Coll Radiol*. 2017; 14 :1027–1033. e2 [PubMed: 28408078]
13. Waddle MR, et al. Photon and proton radiation therapy utilization in a population of more than 100 million commercially insured patients. *Int J Radiat Oncol*. 2017; 99 :1078–1082.
14. Lievens Y, Borrás JM, Grau C. Provision and use of radiotherapy in Europe. *Mol Oncol*. 2020; 14 :1461–1469. [PubMed: 32293084]
15. Particle Therapy Co-Operative Group (PTCOG). Particle therapy facilities in clinical operation. PTCOG. 2021
16. Malouff TD, et al. Carbon ion therapy: a modern review of an emerging technology. *Front Oncol*. 2020; 10 :82. [PubMed: 32117737]
17. Beltran C, Amos RA, Rong Y. We are ready for clinical implementation of carbon ion radiotherapy in the United States. *J Appl Clin Med Phys*. 2020; 21 :6–9.
18. Pompos A, Durante M, Choy H. Heavy ions in cancer therapy. *JAMA Oncol*. 2016; 2 :1539–1540. [PubMed: 27541302]
19. Bortfeld TR, Loeffler JS. Three ways to make proton therapy affordable. *Nature*. 2017; 549 :451–453. [PubMed: 28959981]
20. Jäkel O, Smith AR, Orton CG. The more important heavy charged particle radiotherapy of the future is more likely to be with heavy ions rather than protons. *Med Phys*. 2013; 40 090601 [PubMed: 24007132]
21. Durante M, Debus J. Heavy charged particles: does improved precision and higher biological effectiveness translate to better outcome in patients? *Semin Radiat Oncol*. 2018; 28 :160–167. [PubMed: 29735192]
22. Rackwitz T, Debus J. Clinical applications of proton and carbon ion therapy. *Semin Oncol*. 2019; 46 :226–232. [PubMed: 31451309]
23. Tessonnier T, et al. Helium ions at the heidelberg ion beam therapy center: Comparisons between FLUKA Monte Carlo code predictions and dosimetric measurements. *Phys Med Biol*. 2017; 62 :6784–6803. [PubMed: 28762335]
24. Kurz C, Mairani A, Parodi K. First experimental based characterization of oxygen ion beam depth dose distributions at the Heidelberg Ion-Beam Therapy Center. *Phys Med Biol*. 2012; 57 :5017–5034. [PubMed: 22805295]
25. Kopp B, et al. Development and validation of single field multi-ion particle therapy treatments. *Int J Radiat Oncol*. 2020; 106 :194–205.
26. Inaniwa T, et al. Application of lung substitute material as ripple filter for multi-ion therapy with helium-, carbon-, oxygen-, and neon-ion beams. *Phys Med Biol*. 2021; 66 055002
27. Dokic I, et al. Next generation multi-scale biophysical characterization of high precision cancer particle radiotherapy using clinical proton, helium-, carbon- and oxygen ion beams. *Oncotarget*. 2016; 7 :56676–56689. [PubMed: 27494855]
28. Inaniwa T, et al. Experimental validation of stochastic microdosimetric kinetic model for multi-ion therapy treatment planning with helium-, carbon-, oxygen-, and neon-ion beams. *Phys Med Biol*. 2020; 65 045005 [PubMed: 31968318]
29. Sokol O, Krämer M, Hild S, Durante M, Scifoni E. Kill painting of hypoxic tumors with multiple ion beams. *Phys Med Biol*. 2019; 64 045008 [PubMed: 30641490]
30. Durante M, Paganetti H. Nuclear physics in particle therapy: a review. *Rep Prog Phys*. 2016; 79 096702 [PubMed: 27540827]

31. Newhauser WD, Zhang R. The physics of proton therapy. *Phys Med Biol.* 2015; 60 R155 [PubMed: 25803097]
32. Schardt D, Elsässer T, Schulz-Ertner D. Heavy-ion tumor therapy: physical and radiobiological benefits. *Rev Mod Phys.* 2010; 82 :383–425.
33. Bichsel H. Stochastics of energy loss and biological effects of heavy ions in radiation therapy. *Adv Quantum Chem.* 2013; 65 :1–38.
34. Kamakura S, Sakamoto N, Ogawa H, Tsuchida H, Inokuti M. Mean excitation energies for the stopping power of atoms and molecules evaluated from oscillator-strength spectra. *J Appl Phys.* 2006; 100 064905
35. Bär E, Andreo P, Lalonde A, Royle G, Bouchard H. Optimized I-values for use with the Bragg additivity rule and their impact on proton stopping power and range uncertainty. *Phys Med Biol.* 2018; 63 165007 [PubMed: 29999493]
36. Besemer A, Paganetti H, Bednarz B. The clinical impact of uncertainties in the mean excitation energy of human tissues during proton therapy. *Phys Med Biol.* 2013; 58 :887–902. [PubMed: 23337713]
37. De Smet V, Labarbe R, Vander Stappen F, Macq B, Sterpin E. Reassessment of stopping power ratio uncertainties caused by mean excitation energies using a water-based formalism. *Med Phys.* 2018; 45 :3361–3370. [PubMed: 29729022]
38. Embriaco A, Bellinzona EV, Fontana A, Rotondi A. On Molière and Fermi-Eyges scattering theories in hadrontherapy. *Phys Med Biol.* 2017; 62 :6290–6303. [PubMed: 28714456]
39. Ebrahimi Loushab M, Mowlavi AA, Hadizadeh MH, Izadi R, Jia SB. Impact of various beam parameters on lateral scattering in proton and carbon-ion therapy. *J Biomed Phys Eng.* 2015; 5 :169–176. [PubMed: 26688795]
40. Zeitlin C, La Tessa C. The role of nuclear fragmentation in particle therapy and space radiation protection. *Front Oncol.* 2016; 6 :65. [PubMed: 27065350]
41. Lomax AJ. Myths and realities of range uncertainty. *Br J Radiol.* 2020; 93 20190582 [PubMed: 31778317]
42. Paganetti H. Range uncertainties in proton therapy and the role of Monte Carlo simulations. *Phys Med Biol.* 2012; 57 :R99–R117. [PubMed: 22571913]
43. Durante M, Flanz J. Charged particle beams to cure cancer: strengths and challenges. *Semin Oncol.* 2019; 46 :219–225. [PubMed: 31451308]
44. Knopf A-C, Lomax A. In vivo proton range verification: a review. *Phys Med Biol.* 2013; 58 :R131–R160. [PubMed: 23863203]
45. Parodi K. Vision 20/20: positron emission tomography in radiation therapy planning, delivery, and monitoring. *Med Phys.* 2015; 42 :7153–7168. [PubMed: 26632070]
46. Pönisch F, Parodi K, Hasch BG, Enghardt W. The modelling of positron emitter production and PET imaging during carbon ion therapy. *Phys Med Biol.* 2004; 49 :5217–5232. [PubMed: 15656273]
47. Bauer J, et al. Implementation and initial clinical experience of offline PET/CT-based verification of scanned carbon ion treatment. *Radiother Oncol.* 2013; 107 :218–226. [PubMed: 23647759]
48. Augusto RS, et al. An overview of recent developments in FLUKA PET tools. *Phys Med.* 2018; 54 :189–199. [PubMed: 30017561]
49. Durante M, Parodi K. Radioactive beams in particle therapy: past, present, and future. *Front Phys.* 2020; 8 00326 [PubMed: 33224941]
50. Durante M, Golubev A, Park W-Y, Trautmann C. Applied nuclear physics at the new high-energy particle accelerator facilities. *Phys Rep.* 2019; 800 :1–37.
51. Chacon A, et al. Experimental investigation of the characteristics of radioactive beams for heavy ion therapy. *Med Phys.* 2020; 47 :3123–3132. [PubMed: 32279312]
52. Augusto RS, et al. New developments of <sup>11</sup>C postaccelerated beams for hadron therapy and imaging. *Nucl Instrum Methods Phys Res B.* 2016; 376 :374–378.
53. Chao, AW, Chou, W. *Reviews of Accelerator Science and Technology. Volume 2: Medical Applications of Accelerators.* World Scientific; 2009.

54. Farr JB, Flanz JB, Gerbershagen A, Moyers MF. New horizons in particle therapy systems. *Med Phys.* 2018; 45 :e953–e983. [PubMed: 30421804]
55. Alonso JR, Antaya TA. Superconductivity in medicine. *Rev Accel Sci Technol.* 2012; 05 :227–263.
56. Jongen Y, et al. Compact superconducting cyclotron C400 for hadron therapy. *Nucl Instrum Methods Phys Res A.* 2010; 624 :47–53.
57. Syresin EM, et al. Superconducting synchrotron project for hadron therapy. *Phys Part Nucl Lett.* 2012; 9 :202–212.
58. Noda K, et al. Recent progress and future plans of heavy-ion cancer radiotherapy with HIMAC. *Nucl Instrum Methods Phys Res B.* 2017; 406 :374–378.
59. Zlobin, AV, Schoerling, D. Nb3Sn Accelerator Magnets. Designs, Technologies and Performance. Schoerling, D, Zlobin, A, editors. Springer; 2019. 3–22.
60. Wan W, et al. Alternating-gradient canted cosine theta superconducting magnets for future compact proton gantries. *Phys Rev Spec Top Accel Beams.* 2015; 18 103501
61. Baird YTE, Li Q. Optimized magnetic design of superconducting magnets for heavy ion rotating gantries. *IEEE Trans Appl Supercond.* 2020; 30 :1–8.
62. Caporaso GJ, Chen YJ, Sampayan SE. The dielectric wall accelerator. *Rev Accel Sci Technol.* 2009; 02 :253–263.
63. Ma WJ, et al. Laser acceleration of highly energetic carbon ions using a double-layer target composed of slightly underdense plasma and ultrathin foil. *Phys Rev Lett.* 2019; 122 014803 [PubMed: 31012707]
64. Higginson A, et al. Near-100 MeV protons via a laser-driven transparency-enhanced hybrid acceleration scheme. *Nat Commun.* 2018; 9 724 [PubMed: 29463872]
65. Ahmed H, et al. High energy implementation of coil-target scheme for guided re-acceleration of laser-driven protons. *Sci Rep.* 2021; 11 699 [PubMed: 33436708]
66. Wang KD, et al. Achromatic beamline design for a laser-driven proton therapy accelerator. *Phys Rev Accel Beams.* 2020; 23 111302
67. Karsch L, et al. Towards ion beam therapy based on laser plasma accelerators. *Acta Oncol.* 2017; 56 :1359–1366. [PubMed: 28828925]
68. Linz U, Alonso J. Laser-driven ion accelerators for tumor therapy revisited. *Phys Rev Accel Beams.* 2016; 19 124802
69. Noda K. Progress of radiotherapy technology with HIMAC. *J Phys Conf Ser.* 2019; 1154 012019
70. Kubiak T. Particle therapy of moving targets — the strategies for tumour motion monitoring and moving targets irradiation. *Br J Radiol.* 2016; 89 20150275 [PubMed: 27376637]
71. Bert C, Durante M. Motion in radiotherapy: particle therapy. *Phys Med Biol.* 2011; 56 :R113–R144. [PubMed: 21775795]
72. Riboldi M, Orecchia PR, Baroni PG. Real-time tumour tracking in particle therapy: technological developments and future perspectives. *Lancet Oncol.* 2012; 13 :e383–e391. [PubMed: 22935238]
73. Czarska K, et al. Clinical practice vs. state-of-the-art research and future visions: Report on the 4D treatment planning workshop for particle therapy- Edition 2018 and 2019. *Phys Med.* 2021; 82 :54–63. [PubMed: 33588228]
74. Graeff C, Lüchtenborg R, Eley JG, Durante M, Bert C. A 4D-optimization concept for scanned ion beam therapy. *Radiother Oncol.* 2013; 109 :419–424. [PubMed: 24183865]
75. Iwata Y, et al. Design of a superconducting rotating gantry for heavy-ion therapy. *Phys Rev Spec Top Accel Beams.* 2012; 15 044701
76. Rahim S, et al. Upright radiation therapy — a historical reflection and opportunities for future applications. *Front Oncol.* 2020; 10 :213. [PubMed: 32158693]
77. Yang J, Chu D, Dong L, Court LE. Advantages of simulating thoracic cancer patients in an upright position. *Pract Radiat Oncol.* 2014; 4 :e53–e58. [PubMed: 24621432]
78. Zhang X, et al. Development of an isocentric rotating chair positioner to treat patients of head and neck cancer at upright seated position with multiple nonplanar fields in a fixed carbon-ion beamline. *Med Phys.* 2020; 47 :2450–2460. [PubMed: 32141079]
79. Sheng Y, et al. Performance of a 6D treatment chair for patient positioning in an upright posture for fixed ion beam lines. *Front Oncol.* 2020; 10 :213. [PubMed: 32158693]

80. Cornforth MN. Occam's broom and the dirty DSB: cytogenetic perspectives on cellular response to changes in track structure and ionization density. *Int J Radiat Biol.* 2020; 97 :1099–1108. [PubMed: 31971454]
81. Stannard C, et al. Malignant salivary gland tumours: can fast neutron therapy results point the way to carbon ion therapy? *Radiother Oncol.* 2013; 109 :262–268. [PubMed: 24044797]
82. Parker C, et al. Targeted alpha therapy, an emerging class of cancer agents. *JAMA Oncol.* 2018; 4 :1765–1772. [PubMed: 30326033]
83. Durante M, Orecchia R, Loeffler JS. Charged-particle therapy in cancer: clinical uses and future perspectives. *Nat Rev Clin Oncol.* 2017; 14 :483–495. [PubMed: 28290489]
84. Blakely EA. The 20th Gray lecture 2019: health and heavy ions. *Br J Radiol.* 2020; 93 20200172 [PubMed: 33021811]
85. Fowler JF. 21 years of biologically effective dose. *Br J Radiol.* 2010; 83 :554–568. [PubMed: 20603408]
86. Friedrich T, Scholz U, Elsässer T, Durante M, Scholz M. Systematic analysis of RBE and related quantities using a database of cell survival experiments with ion beam irradiation. *J Radiat Res.* 2013; 54 :494–514. [PubMed: 23266948]
87. Wang JZ, Huang Z, Lo SS, Yuh WTC, Mayr NA. A generalized linear-quadratic model for radiosurgery, stereotactic body radiation therapy, and high-dose rate brachytherapy. *Sci Transl Med.* 2010; 2 39ra48
88. Takahashi Y, et al. Heavy ion irradiation inhibits in vitro angiogenesis even at sublethal dose. *Cancer Res.* 2003; 63 :4253–4257. [PubMed: 12874034]
89. Liu Y, et al. Effects of carbon-ion beam irradiation on the angiogenic response in lung adenocarcinoma A549 cells. *Cell Biol Int.* 2014; 38 :1304–1310. [PubMed: 24942319]
90. Konings K, Vandevoorde C, Baselet B, Baatout S, Moreels M. Combination therapy with charged particles and molecular targeting: a promising avenue to overcome radioresistance. *Front Oncol.* 2020; 10 :128. [PubMed: 32117774]
91. Durante M, Brenner DJ, Formenti SC. Does heavy ion therapy work through the immune system? *Int J Radiat Oncol Biol Phys.* 2016; 96 :934–936. [PubMed: 27869095]
92. Wulf H, et al. Heavy-ion effects on mammalian cells: inactivation measurements with different cell lines. *Radiat Res.* 1985; 104 :122–134.
93. ICRU Report 93: Prescribing, Recording, and Reporting Light Ion Beam Therapy. *J ICRU.* 2016; 16
94. Inaniwa T, et al. Treatment planning for a scanned carbon beam with a modified microdosimetric kinetic model. *Phys Med Biol.* 2010; 55 :6721–6737. [PubMed: 21030747]
95. Grün R, et al. Impact of enhancements in the local effect model (LEM) on the predicted RBE-weighted target dose distribution in carbon ion therapy. *Phys Med Biol.* 2012; 57 :7261–7274. [PubMed: 23075883]
96. Tommasino F, Durante M. Proton radiobiology. *Cancers.* 2015; 7 :353–381. [PubMed: 25686476]
97. Paganetti H. Relative biological effectiveness (RBE) values for proton beam therapy. Variations as a function of biological endpoint, dose, and linear energy transfer. *Phys Med Biol.* 2014; 59 :R419–R472. [PubMed: 25361443]
98. Mutter RW, et al. Incorporation of biologic response variance modeling into the clinic: limiting risk of brachial plexopathy and other late effects of breast cancer proton beam therapy. *Pract Radiat Oncol.* 2020; 10 :e71–e81. [PubMed: 31494289]
99. Zhang L, Wang W, Hu J, Lu J, Kong L. RBE-weighted dose conversions for patients with recurrent nasopharyngeal carcinoma receiving carbon-ion radiotherapy from the local effect model to the microdosimetric kinetic model. *Radiat Oncol.* 2020; 15 :277. [PubMed: 33302998]
100. Wang W, et al. RBE-weighted dose conversions for carbon ionradiotherapy between microdosimetric kinetic model and local effect model for the targets and organs at risk in prostate carcinoma. *Radiother Oncol.* 2020; 144 :30–36. [PubMed: 31710941]
101. Molinelli S, et al. Dose prescription in carbon ion radiotherapy: How to compare two different RBE-weighted dose calculation systems. *Radiother Oncol.* 2016; 120 :307–312. [PubMed: 27394694]



102. Fossati P, Matsufuji N, Kamada T, Karger CP. Radiobiological issues in prospective carbon ion therapy trials. *Med Phys.* 2018; 45 :e1096–e1110. [PubMed: 30421806]
103. Friedrich T, Scholz U, Durante M, Scholz M. RBE of ion beams in hypofractionated radiotherapy (SBRT). *Phys Med.* 2014; 30 :588–591. [PubMed: 24857333]
104. Yoshida Y, et al. Evaluation of therapeutic gain for fractionated carbon-ion radiotherapy using the tumor growth delay and crypt survival assays. *Radiother Oncol.* 2015; 117 :351–357. [PubMed: 26454348]
105. Chapman JD. Can the two mechanisms of tumor cell killing by radiation be exploited for therapeutic gain? *J Radiat Res.* 2014; 55 :2–9. [PubMed: 24105710]
106. Laine AM, et al. The role of hypofractionated radiation therapy with photons, protons, and heavy ions for treating extracranial lesions. *Front Oncol.* 2016; 5 :302. [PubMed: 26793619]
107. Barker HE, Paget JTE, Khan AA, Harrington KJ. The tumour microenvironment after radiotherapy: mechanisms of resistance and recurrence. *Nat Rev Cancer.* 2015; 15 :409–425. [PubMed: 26105538]
108. Strigari L, Benassi M, Sarnelli A, Polico R, D'Andrea M. A modified hypoxia-based TCP model to investigate the clinical outcome of stereotactic hypofractionated regimes for early stage non-small-cell lung cancer (NSCLC). *Med Phys.* 2012; 39 :4502–4514. [PubMed: 22830782]
109. Toma-Dasu I, Sandström H, Barsoum P, Dasu A. To fractionate or not to fractionate? That is the question for the radiosurgery of hypoxic tumors. *J Neurosurg.* 2014; 121 :110–115. [PubMed: 25434944]
110. Mc Keown SR. Defining normoxia, physoxia and hypoxia in tumours — implications for treatment response. *Br J Radiol.* 2014; 87 20130676 [PubMed: 24588669]
111. Furusawa Y, et al. Inactivation of aerobic and hypoxic cells from three different cell lines by accelerated (3) He-, (12)C- and (20)Ne-ion beams. *Radiat Res.* 2000; 154 :485–496. [PubMed: 11025645]
112. Tinganelli W, et al. Kill-painting of hypoxic tumours in charged particle therapy. *Sci Rep.* 2015; 5 17016 [PubMed: 26596243]
113. Grassberger C, Ellsworth SG, Wilks MQ, Keane FK, Loeffler JS. Assessing the interactions between radiotherapy and antitumour immunity. *Nat Rev Clin Oncol.* 2019; 16 :729–745. [PubMed: 31243334]
114. Durante M, et al. X-rays vs. carbon-ion tumor therapy: cytogenetic damage in lymphocytes. *Int J Radiat Oncol Biol Phys.* 2000; 47 :793–798. [PubMed: 10837966]
115. Durante M, Formenti S. Harnessing radiation to improve immunotherapy: better with particles? *Br J Radiol.* 2020; 93 20190224 [PubMed: 31317768]
116. Davuluri R, et al. Lymphocyte nadir and esophageal cancer survival outcomes after chemoradiation therapy. *Int J Radiat Oncol.* 2017; 99 :128–135.
117. Mohan R, et al. Proton therapy reduces the likelihood of high-grade radiation-induced lymphopenia in glioblastoma patients: phase II randomized study of protons vs photons. *Neuro Oncol.* 2021; 23 :284–294. [PubMed: 32750703]
118. Kim N, et al. Proton beam therapy reduces the risk of severe radiation-induced lymphopenia during chemoradiotherapy for locally advanced non-small cell lung cancer: a comparative analysis of proton versus photon therapy. *Radiother Oncol.* 2021; 156 :166–173. [PubMed: 33359267]
119. Takahashi Y, et al. Carbon ion irradiation enhances the antitumor efficacy of dual immune checkpoint blockade therapy both for local and distant sites in murine osteosarcoma. *Oncotarget.* 2019; 10 :633–646. [PubMed: 30774761]
120. Helm A, et al. Reduction of lung metastases in a mouse osteosarcoma model treated with carbon ions and immune checkpoint inhibitors. *Int J Radiat Oncol.* 2021; 109 :594–602.
121. Marcus D, et al. Charged particle and conventional radiotherapy: current implications as partner for immunotherapy. *Cancers.* 2021; 13 :1468. [PubMed: 33806808]
122. Friedrich T, Henthorn N, Durante M. Modeling radioimmune response — current status and perspectives. *Front Oncol.* 2021; 11 647272 [PubMed: 33796470]
123. Wang Z, et al. Charged particle radiation therapy for uveal melanoma: a systematic review and meta-analysis. *Int J Radiat Oncol.* 2013; 86 :18–26.

124. Mishra KK, et al. Long-term results of the UCSF- LBNL randomized trial: charged particle with helium ion versus iodine-125 plaque therapy for choroidal and ciliary body melanoma. *Int J Radiat Oncol Biol Phys.* 2015; 92 :376–383. [PubMed: 25841624]
125. Kamada T, et al. Carbon ion radiotherapy in Japan: an assessment of 20 years of clinical experience. *Lancet Oncol.* 2015; 16 :e93–e100. [PubMed: 25638685]
126. Shinoto M, et al. Carbon ion radiation therapy with concurrent gemcitabine for patients with locally advanced pancreatic cancer. *Int J Radiat Oncol Biol Phys.* 2016; 95 :498–504. [PubMed: 26883565]
127. Kawashiro S, et al. Multi-institutional study of carbonion radiotherapy for locally advanced pancreatic cancer: Japan Carbon-ion Radiation Oncology Study Group (J-CROS) study 1403 pancreas. *Int J Radiat Oncol.* 2018; 101 :1212–1221.
128. Nevala-Plagemann C, Hidalgo M, Garrido-Laguna I. From state-of-the-art treatments to novel therapies for advanced-stage pancreatic cancer. *Nat Rev Clin Oncol.* 2020; 17 :108–123. [PubMed: 31705130]
129. Yamasaki A, Yanai K, Onishi H. Hypoxia and pancreatic ductal adenocarcinoma. *Cancer Lett.* 2020; 484 :9–15. [PubMed: 32380129]
130. Ho WJ, Jaffee EM, Zheng L. The tumour microenvironment in pancreatic cancer — clinical challenges and opportunities. *Nat Rev Clin Oncol.* 2020; 17 :527–540. [PubMed: 32398706]
131. Huart C, Chen J, Le Calvé B, Michiels C, Wéra AC. Could protons and carbon ions be the silver bullets against pancreatic cancer? *Int J Mol Sci.* 2020; 21 :4767.
132. Liermann J, et al. Carbon ion radiotherapy in pancreatic cancer: a review of clinical data. *Radiother Oncol.* 2020; 147 :145–150. [PubMed: 32416281]
133. Dreher C, Habermehl D, Jäkel O, Combs SE. Effective radiotherapeutic treatment intensification in patients with pancreatic cancer: higher doses alone, higher RBE or both? *Radiat Oncol.* 2017; 12 :203. [PubMed: 29282139]
134. Shinoto M, et al. Carbon-ion radiotherapy for locally recurrent rectal cancer: Japan Carbon-ion Radiation Oncology Study Group (J-CROS) study 1404 rectum. *Radiother Oncol.* 2019; 132 :236–240. [PubMed: 30360998]
135. Cai X, et al. The role of carbon ion radiotherapy for unresectable locally recurrent rectal cancer: a single institutional experience. *Radiat Oncol.* 2020; 15 :209. [PubMed: 32859234]
136. Habermehl D, et al. Reirradiation using carbon ions in patients with locally recurrent rectal cancer at HIT: first results. *Ann Surg Oncol.* 2015; 22 :2068–2074. [PubMed: 25384705]
137. Guren MG, et al. Reirradiation of locally recurrent rectal cancer: a systematic review. *Radiother Oncol.* 2014; 113 :151–157. [PubMed: 25613395]
138. Venkatesulu BP, Giridhar P, Malouf TD, Trifletti DM, Krishnan S. A systematic review of the role of carbon ion radiation therapy in recurrent rectal cancer. *Acta Oncol.* 2020; 59 :1218–1223. [PubMed: 32476538]
139. Imada H, et al. Comparison of efficacy and toxicity of short-course carbon ion radiotherapy for hepatocellular carcinoma depending on their proximity to the porta hepatis. *Radiother Oncol.* 2010; 96 :231–235. [PubMed: 20579756]
140. Qi W-X, Fu S, Zhang Q, Guo XM. Charged particle therapy versus photon therapy for patients with hepatocellular carcinoma: a systematic review and meta-analysis. *Radiother Oncol.* 2015; 114 :289–295. [PubMed: 25497556]
141. Habermehl D, et al. Hypofractionated carbon ion therapy delivered with scanned ion beams for patients with hepatocellular carcinoma-feasibility and clinical response. *Radiat Oncol.* 2013; 8 :59. [PubMed: 23497349]
142. Shibuya K, et al. A feasibility study of high-dose hypofractionated carbon ion radiation therapy using four fractions for localized hepatocellular carcinoma measuring 3 cm or larger. *Radiother Oncol.* 2019; 132 :230–235. [PubMed: 30366726]
143. Chauvel P. Osteosarcomas and adult soft tissue sarcomas: is there a place for high LET radiation therapy? *Ann Oncol.* 1992; 3 :S107–S110. [PubMed: 1622850]
144. Strander H, Turesson I, Cavallin-ståhl E. A systematic overview of radiation therapy effects in soft tissue sarcomas. *Acta Oncol.* 2003; 42 :516–531. [PubMed: 14596510]

145. Weber DC, et al. Profile of European proton and carbon ion therapy centers assessed by the EORTC facility questionnaire. *Radiother Oncol.* 2017; 124 :185–189. [PubMed: 28764925]
146. Matsunobu A, et al. Impact of carbon ion radiotherapy for unresectable osteosarcoma of the trunk. *Cancer.* 2012; 118 :4555–4563. [PubMed: 22359113]
147. Kamada T, et al. Efficacy and safety of carbon ion radiotherapy in bone and soft tissue sarcomas. *J Clin Oncol.* 2002; 20 :4466–4471. [PubMed: 12431970]
148. Cuccia F, et al. Outcome and toxicity of carbon ion radiotherapy for axial bone and soft tissue sarcomas. *Anticancer Res.* 2020; 40 :2853–2859. [PubMed: 32366434]
149. Seidensaal K, et al. The role of combined ion-beam radiotherapy (CIBRT) with protons and carbon ions in a multimodal treatment strategy of inoperable osteosarcoma. *Radiother Oncol.* 2021; 159 :8–16. [PubMed: 33549644]
150. Uhl M, et al. Highly effective treatment of skull base chordoma with carbon ion irradiation using a raster scan technique in 155 patients: first long-term results. *Cancer.* 2014; 120 :3410–3417. [PubMed: 24948519]
151. Mattke M, et al. High control rates of proton- and carbon-ion-beam treatment with intensity-modulated active raster scanning in 101 patients with skull base chondrosarcoma at the Heidelberg Ion Beam Therapy Center. *Cancer.* 2018; 124 :2036–2044. [PubMed: 29469932]
152. Nikoghosyan AV, et al. Randomised trial of proton vs. carbon ion radiation therapy in patients with low and intermediate grade chondrosarcoma of the skull base, clinical phase III study. *BMC Cancer.* 2010; 10 :606. [PubMed: 21050498]
153. Cramer JD, Burtness B, Le QT, Ferris RL. The changing therapeutic landscape of head and neck cancer. *Nat Rev Clin Oncol.* 2019; 16 :669–683. [PubMed: 31189965]
154. Akbaba S, et al. Bimodal radiotherapy with active raster-scanning carbon ion radiotherapy and intensity-modulated radiotherapy in high-risk nasopharyngeal carcinoma results in excellent local control. *Cancers.* 2019; 11 :379.
155. Shirai K, et al. Prospective observational study of carbon-ion radiotherapy for non-squamous cell carcinoma of the head and neck. *Cancer Sci.* 2017; 108 :2039–2044. [PubMed: 28730646]
156. Högerle BA, et al. Primary adenoid cystic carcinoma of the trachea: clinical outcome of 38 patients after interdisciplinary treatment in a single institution. *Radiat Oncol.* 2019; 14 :117. [PubMed: 31272473]
157. Kong L, et al. Phase I/II trial evaluating carbon ion radiotherapy for salvaging treatment of locally recurrent nasopharyngeal carcinoma. *J Cancer.* 2016; 7 :774–783. [PubMed: 27162535]
158. Baumann BC, et al. Comparative effectiveness of proton vs photon therapy as part of concurrent chemoradiotherapy for locally advanced cancer. *JAMA Oncol.* 2020; 6 :237–246. [PubMed: 31876914]
159. Li X, et al. Toxicity profiles and survival outcomes among patients with nonmetastatic nasopharyngeal carcinoma treated with intensity-modulated proton therapy vs intensity-modulated radiation therapy. *JAMA Netw Open.* 2021; 4 e2113205 [PubMed: 34143193]
160. Gondi V, Yock TI, Mehta MP. Proton therapy for paediatric CNS tumours — improving treatment-related outcomes. *Nat Rev Neurol.* 2016; 12 :334–345. [PubMed: 27197578]
161. Newhauser WD, Durante M. Assessing the risk of second malignancies after modern radiotherapy. *Nat Rev Cancer.* 2011; 11 :438–448. [PubMed: 21593785]
162. Rieber JG, et al. Treatment tolerance of particle therapy in pediatric patients. *Acta Oncol.* 2015; 54 :1049–1055. [PubMed: 25615893]
163. Mohamad O, et al. Risk of subsequent primary cancers after carbon ion radiotherapy, photon radiotherapy, or surgery for localised prostate cancer: a propensity score-weighted, retrospective, cohort study. *Lancet Oncol.* 2019; 20 :674–685. [PubMed: 30885458]
164. Ohno T, Okamoto M. Carbon ion radiotherapy as a treatment modality for paediatric cancers. *Lancet Child Adolesc Health.* 2019; 3 :371–372. [PubMed: 30948250]
165. Knäusel B, Fuchs H, Dieckmann K, Georg D. Can particle beam therapy be improved using helium ions? - A planning study focusing on pediatric patients. *Acta Oncol.* 2016; 55 :751–759. [PubMed: 26750803]
166. Horst F, et al. Physical characterization of <sup>3</sup>He ion beams for radiotherapy and comparison with <sup>4</sup>He. *Phys Med Biol.* 2021; 66 095009

167. Tommasino F, Scifoni E, Durante M. New ions for therapy. *Int J Part Ther.* 2015; 2 :428–438.
168. Scifoni E, et al. Including oxygen enhancement ratio in ion beam treatment planning: model implementation and experimental verification. *Phys Med Biol.* 2013; 58 :3871–3895. [PubMed: 23681217]
169. Sokol O, et al. Oxygen beams for therapy: advanced biological treatment planning and experimental verification. *Phys Med Biol.* 2017; 62 :7798–7813. [PubMed: 28841579]
170. Hagiwara Y, et al. Influence of dose-averaged linear energy transfer on tumour control after carbon-ion radiation therapy for pancreatic cancer. *Clin Transl Radiat Oncol.* 2020; 21 :19–24. [PubMed: 31886424]
171. Matsumoto S, et al. Unresectable chondrosarcomas treated with carbon ion radiotherapy: relationship between dose-averaged linear energy transfer and local recurrence. *Anticancer Res.* 2020; 40 :6429–6435. [PubMed: 33109581]
172. Bassler N, et al. LET-painting increases tumour control probability in hypoxic tumours. *Acta Oncol.* 2014; 53 :25–32. [PubMed: 24020629]
173. Bassler N, Jäkel O, Søndergaard CS, Petersen JB. Dose- and LET-painting with particle therapy. *Acta Oncol.* 2010; 49 :1170–1176. [PubMed: 20831510]
174. Ebner DK, Frank SJ, Inaniwa T, Yamada S, Shirai T. The emerging potential of multi-ion radiotherapy. *Front Oncol.* 2021; 11 624786 [PubMed: 33692957]
175. Inaniwa T, Kanematsu N, Noda K, Kamada T. Treatment planning of intensity modulated composite particle therapy with dose and linear energy transfer optimization. *Phys Med Biol.* 2017; 62 :5180–5197. [PubMed: 28333688]
176. Horsman MR, et al. Imaging hypoxia to improve radiotherapy outcome. *Nat Rev Clin Oncol.* 2012; 9 :674–687. [PubMed: 23149893]
177. Mazal A, et al. FLASH and minibeam radiation therapy: the effect of microstructures on time and space and their potential application to proton therapy. *Br J Radiol.* 2020; 93 20190807 [PubMed: 32003574]
178. Favaudon V, et al. Ultrahigh dose-rate FLASH irradiation increases the differential response between normal and tumor tissue in mice. *Sci Transl Med.* 2014; 6 245ra93
179. Vozenin MC, et al. The advantage of FLASH radiotherapy confirmed in mini-pig and cat-cancer patients. *Clin Cancer Res.* 2019; 25 :35–42. [PubMed: 29875213]
180. Montay-Gruel P, et al. Hypofractionated FLASH-RT as an effective treatment against glioblastoma that reduces neurocognitive side effects in mice. *Clin Cancer Res.* 2021; 27 :775–784. [PubMed: 33060122]
181. Di Martino F, et al. FLASH radiotherapy with electrons: issues related to the production, monitoring, and dosimetric characterization of the beam. *Front Phys.* 2020; 8 570697
182. Jolly S, Owen H, Schippers M, Welsch C. Technical challenges for FLASH proton therapy. *Phys Med.* 2020; 78 :71–82. [PubMed: 32947086]
183. Zakaria AM, et al. Ultra-high dose-rate, pulsed (FLASH) radiotherapy with carbon ions: generation of early, transient, highly oxygenated conditions in the tumor environment. *Radiat Res.* 2020; 194 :587–593. [PubMed: 32853343]
184. Vozenin M-C, Montay-Gruel P, Limoli C, Germond J-F. All irradiations that are ultra-high dose rate may not be FLASH: the critical importance of beam parameter characterization and in vivo validation of the FLASH effect. *Radiat Res.* 2020; 194 :571–572. [PubMed: 32853355]
185. Rothwell BC, et al. Determining the parameter space for effective oxygen depletion for FLASH radiation therapy. *Phys Med Biol.* 2021; 66 055020
186. Chaudhary P, et al. Radiobiology experiments with ultra-high dose rate laser-driven protons: methodology and state-of-the-art. *Front Phys.* 2021; 9 624963
187. Bourhis J, et al. Treatment of a first patient with FLASH-radiotherapy. *Radiother Oncol.* 2019; 139 :18–22. [PubMed: 31303340]
188. Prax G, Kapp DS. A computational model of radiolytic oxygen depletion during FLASH irradiation and its effect on the oxygen enhancement ratio. *Phys Med Biol.* 2019; 64 185005 [PubMed: 31365907]

189. Labarbe R, Hotoiu L, Barbier J, Favaudon V. A physicochemical model of reaction kinetics supports peroxy radical recombination as the main determinant of the FLASH effect. *Radiother Oncol.* 2020; 153 :303–310. [PubMed: 32534957]
190. Jansen J, et al. Does FLASH deplete oxygen? Experimental evaluation for photons, protons, and carbon ions. *Med Phys.* 2021; 48 :3982–3990. [PubMed: 33948958]
191. Boscolo D, Scifoni E, Durante M, Krämer M, Fuss MC. May oxygen depletion explain the FLASH effect? A chemical track structure analysis. *Radiother Oncol.* 2021; 162 :68–75. [PubMed: 34214612]
192. Weber U, Scifoni E, Durante M. FLASH radiotherapy with carbon ion beams. *Med Phys.* 2021; doi: 10.1002/mp.15135
193. Schültke E, et al. Microbeam radiation therapy — grid therapy and beyond: a clinical perspective. *Br J Radiol.* 2017; 90 20170073 [PubMed: 28749174]
194. Lamirault C, et al. Short and long-term evaluation of the impact of proton minibeam radiation therapy on motor, emotional and cognitive functions. *Sci Rep.* 2020; 10 13511 [PubMed: 32782370]
195. Billena C, Khan AJ. A current review of spatial fractionation: back to the future. *Int J Radiat Oncol.* 2019; 104 :177–187.
196. Dilmanian FA, et al. Interlaced x-ray microplanar beams: a radiosurgery approach with clinical potential. *Proc Natl Acad Sci USA.* 2006; 103 :9709–9714. [PubMed: 16760251]
197. Dilmanian FA, et al. Interleaved carbon minibeam: an experimental radiosurgery method with clinical potential. *Int J Radiat Oncol Biol Phys.* 2012; 84 :514–519. [PubMed: 22342299]
198. González W, Prezado Y. Spatial fractionation of the dose in heavy ions therapy: an optimization study. *Med Phys.* 2018; 45 :2620–2627. [PubMed: 29633284]
199. Prezado Y, et al. A potential renewed use of very heavy ions for therapy: neon minibeam radiation therapy. *Cancers.* 2021; 12 :1356.
200. Kirkby KJ, et al. Heavy charged particle beam therapy and related new radiotherapy technologies: the clinical potential, physics and technical developments required to deliver benefit for patients with cancer. *Br J Radiol.* 2020; 93 20200247 [PubMed: 33021102]
201. Kramer M, et al. Helium ions for radiotherapy? Physical and biological verifications of a novel treatment modality. *Med Phys.* 2016; 43 :1995–2004. [PubMed: 27036594]

**Hypoxia**

Reduced oxygen supply in a tissue compared with the normal level (normoxia or physioxia). Tumours are typically hypoxic.

**Linear energy transfer**

Energy loss of charged particles per unit track length (see Eq. 1).

**Spread-out Bragg peak**

The monoenergetic beam Bragg peak is too narrow to cover a tumour volume. It must, therefore, be enlarged to provide a uniform biological dose to the target volume.

**Track structure**

The complete set of ionizations and excitation events caused by a charged particle traversing a medium. Energy is deposited either directly by the traversing ion or by the high-energy electrons emitted by target atom ionization ( $\delta$ -rays — see Supplementary Video 1).

**Conformal radiotherapy**

A delivery system that shapes the radiation beams to match the shape of the tumour.

**Straggling**

Variation in the range of a particle beam caused by the stochastic nature of the energy loss process.

**Dose halo**

Energy deposited due to scattering in the volume immediately surrounding the target.

**Treatment planning**

The calculation of the optimal beam directions, energies and intensities to achieve the highest possible dose to the tumour while sparing organs at risk and reducing unnecessary dose to the normal tissue.

**Hypofractionation**

Reduction of the number of fractions and increase of the dose per fraction compared with the conventional radiotherapy scheme (2 Gy per fraction in 20–30 fractions, one fraction per day).

**Gyroradius**

Radius of the circular motion of a charged particle in the presence of a uniform magnetic field.

**Rigidity**

Impact of the magnetic field on the trajectory of a charged particle (Eq. 5).

**Passive modulation systems**



Systems to produce spread-out Bragg peak from a monoenergetic beam using passive scatterers with different techniques, such as a rotating wheel of different techniques or a scatterer with a collimator and a patient-specific compensator.

#### **Targeted radioimmunotherapy**

Cancer therapy that uses a targeting construct (e.g. antibody, peptides or nanoparticles), attached to a radionuclide, to deliver a systemic cytotoxic dose of radiation to malignant tissue.

#### **Reoxygenation**

Hypoxic sub-volumes in cancers are radioresistant. During the interval between fractions, the blood can reach the hypoxic niches that survived the previous fraction, making them radiosensitive.

#### **second cancers**

malignant neoplasias induced by the treatment to a primary tumour.

### Key points

- Charged particle therapy is the most advanced radiotherapy technique.
- Most of the patients are treated with protons, but heavy ions present additional biological advantages.
- Carbon-ion therapy is ongoing in 12 centres worldwide and clinical results are promising, whereas new ions (like  $^4\text{He}$  and  $^{16}\text{O}$ ) will be used in the future.
- Heavy ion therapy is much more expensive than X-ray therapy and level 1 evidence of superiority is missing.
- Radiobiology suggests that heavy ions can be exquisitely effective against hypoxic tumours and improve the effects of immunotherapy.
- Rather than a ‘silver bullet’, different particles and their combination can provide optimal results in specific cases.

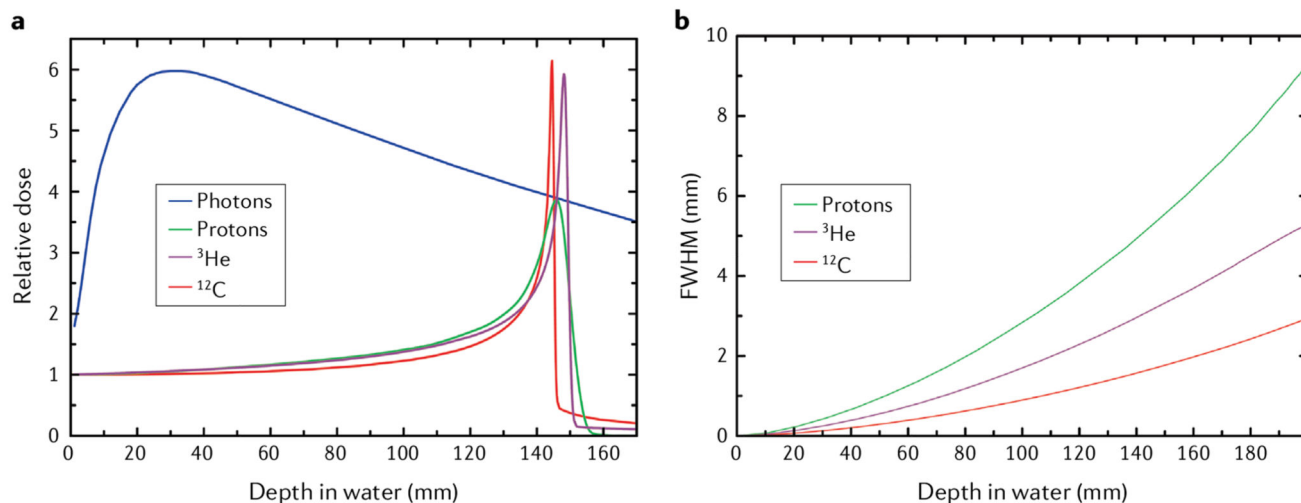


### Figure 1. Heavy ion physics

**a** | Depth-dose distributions showing the Bragg peak for different ions and the reduced straggling of heavier ions. The X-ray depth-dose curve is calculated for a high-energy 21-MeV linac. Energies of the ions correspond approximately to the same range (15 cm in tissue): 148 MeV $^1\text{H}$  beam, 170 MeV/n $^3\text{He}$  beam and 270 MeV/n $^{12}\text{C}$  beam. **b** | Lateral broadening (full width at half maximum (FWHM) of the Gaussian distribution, see Eq. 3) for the same ions. The widening of the beam should be compared with typical entrance spot sizes of proton and ion beams of ~5–10 mm. Image from the GSI image gallery, distributed under Creative Commons CC-BY. Figure is adapted from REF.<sup>201</sup>, [CC BY 4.0](#).

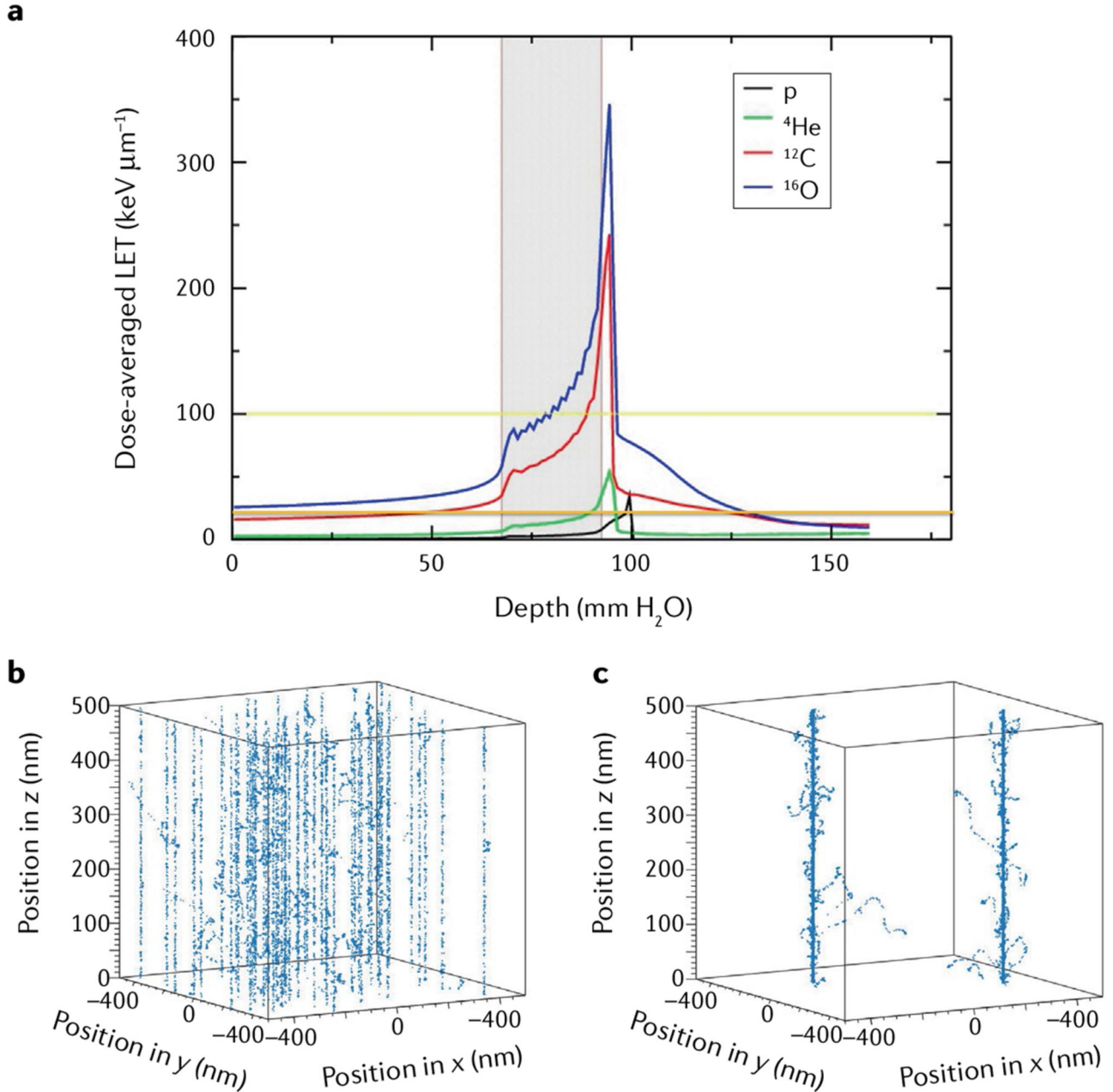


**Figure 2. Dose-averaged linear energy transfer versus depth in tissue for a single spread-out Bragg peak of protons, He, C and O providing a uniform physical dose (2 Gy) in the target volume.**

**a** | The grey area represents the tumour region, a  $2.5 \times 2.5 \times 2.5 \text{ cm}^3$  volume centred at 8 cm in water. The yellow and orange lines are 100 and 20  $\text{keV } \mu\text{m}^{-1}$  linear energy transfer (LET) levels, respectively. An ideal bullet should have  $\text{LET} < 20 \text{ keV } \mu\text{m}^{-1}$  in the entrance channel and  $> 100 \text{ keV } \mu\text{m}^{-1}$  in the target volume<sup>7</sup>. **b,c** | Monte Carlo TRAX code simulation of C-ion tracks in the entrance channel (100 MeV/n; to the left of the grey tumour region in part **a**) and the Bragg peak (3 MeV/n), providing the same dose in a  $1 \times 1 \times 0.5 \mu\text{m}^3$  volume.

Figure modified from Tommasino et al.<sup>167</sup>, distributed under Creative Commons CC-BY.  
Part a is adapted from REF.<sup>167</sup>, [CC BY 4.0](#).

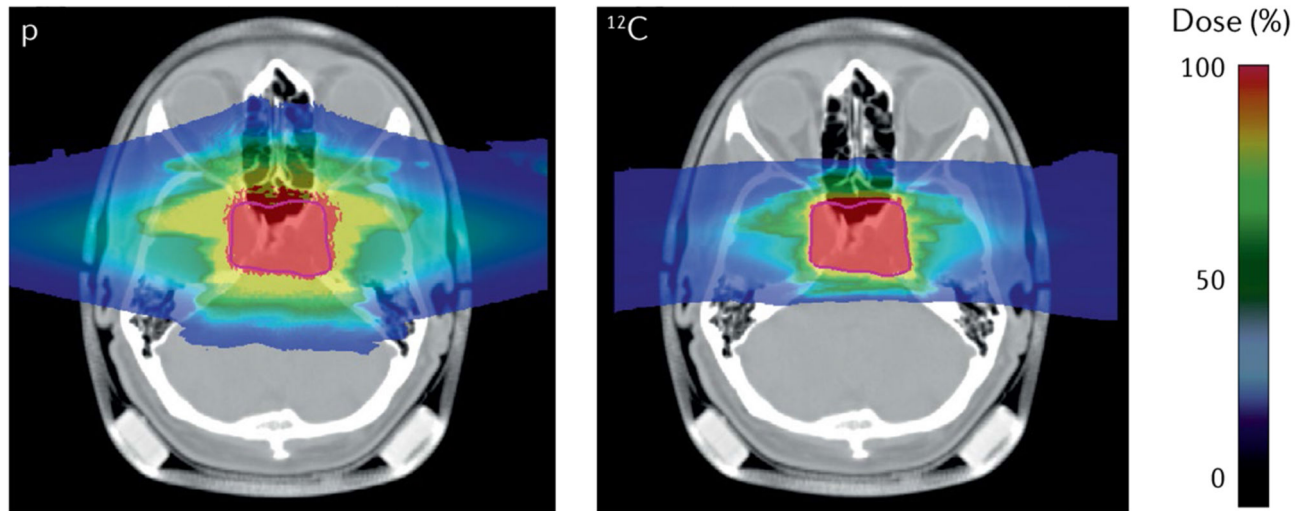


**Figure 3. Impact of lateral scattering on treatment planning.**

The image shows an optimized plan with two opposite fields for a chordoma patient using protons (left) or  $^{12}\text{C}$  ions (right). Colour scale represents the delivered relative biological effectiveness-weighted dose relative to the target dose of 2 Gy, prescribed to the planning target volume (purple line). The dose halo in the proton plan is caused by the larger lateral scattering of the light protons compared with the heavier carbon nuclei. Image from the GSI patient project archive, distributed under Creative Commons [CC BY 4.0](https://creativecommons.org/licenses/by/4.0/).



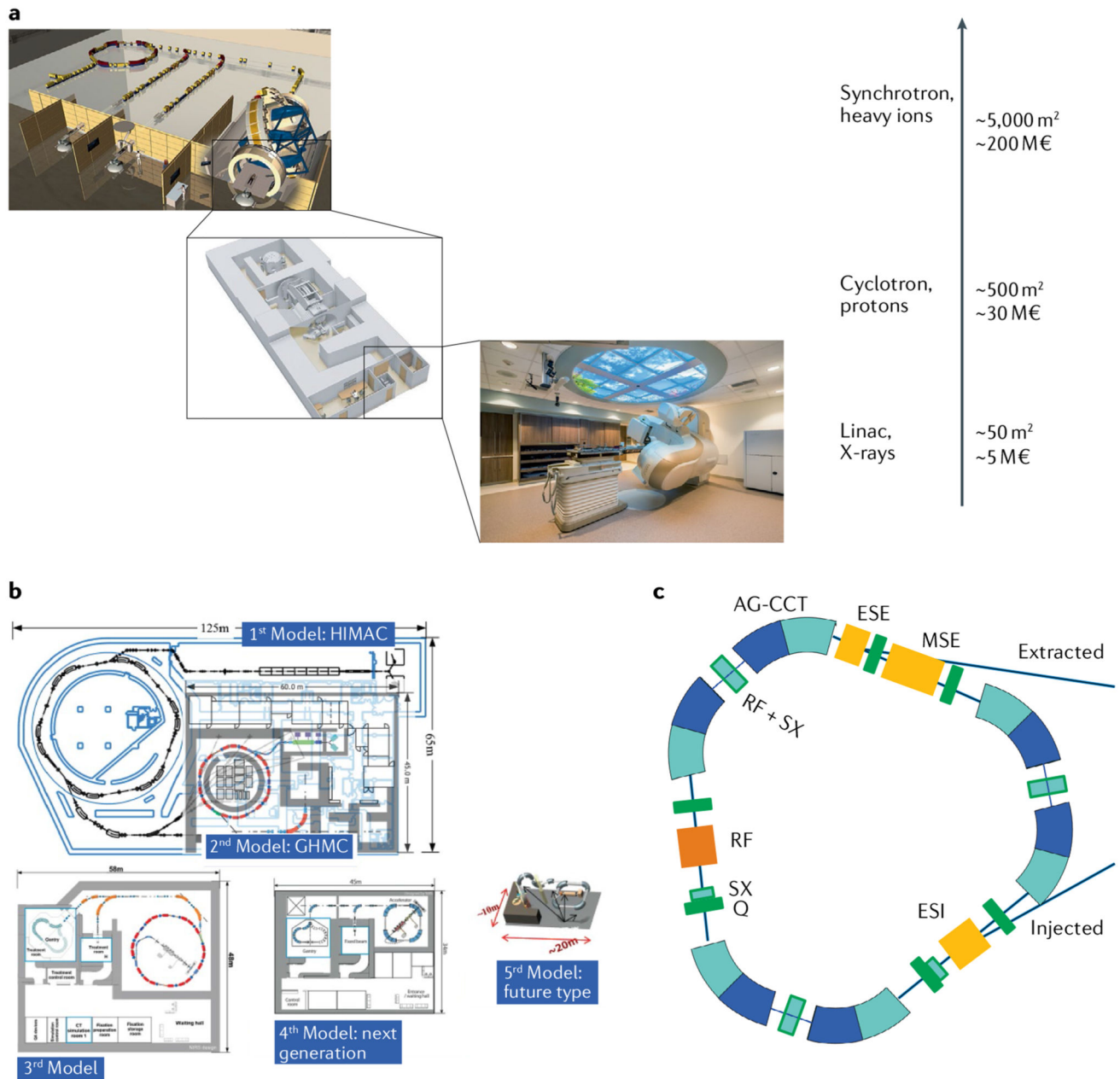


**Figure 4. Accelerator technologies in heavy ion therapy.**

**a** | The impact of advancing technology on footprint and costs of radiotherapy facilities. Size and prices can have large variation, but the image gives an indication of the increase in footprint and price. **b** | Plans at the National Institutes for Quantum and Radiological Science and Technology (NIRS-QST, Chiba, Japan) for reducing the footprint of heavy ion centres. The image shows the large research Heavy-Ion Medical Accelerator (HIMAC) and the subsequent concepts already implemented (such as the Gunma facility) or under development. GHMC, Gunma University Heavy Ion Medical Center. Image courtesy of K. Noda, NIRS-QST. **c** | An innovative concept of a superconducting synchrotron for heavy

ion therapy developed at CERN. The triangular accelerator with a 3.5-T superconducting magnet is capable of accelerating C ions up to 430 MeV/n with  $10^{10}$  ions per pulse in a footprint approximately one-quarter of the present-day resistive magnet medical synchrotrons in part **b**. AG-CCT, alternating gradient canted cosine theta; ESE, electrostatic extraction septum; ESI, electrostatic injection septum; MSE, magnetic extraction septum; Q, quadrupole magnet; RF, radiofrequency cavity; SX, sextupole magnet. Image and information courtesy of Elena Benedetto, CERN & TERA Foundation. Part **a** with permission from © GSI Helmholtzzentrum für Schwerionenforschung GmbH. Part **b**, image courtesy of Dr Koichi Noda. Part **c**, image courtesy of Elena Benedetto, TERA Foundation and CERN.

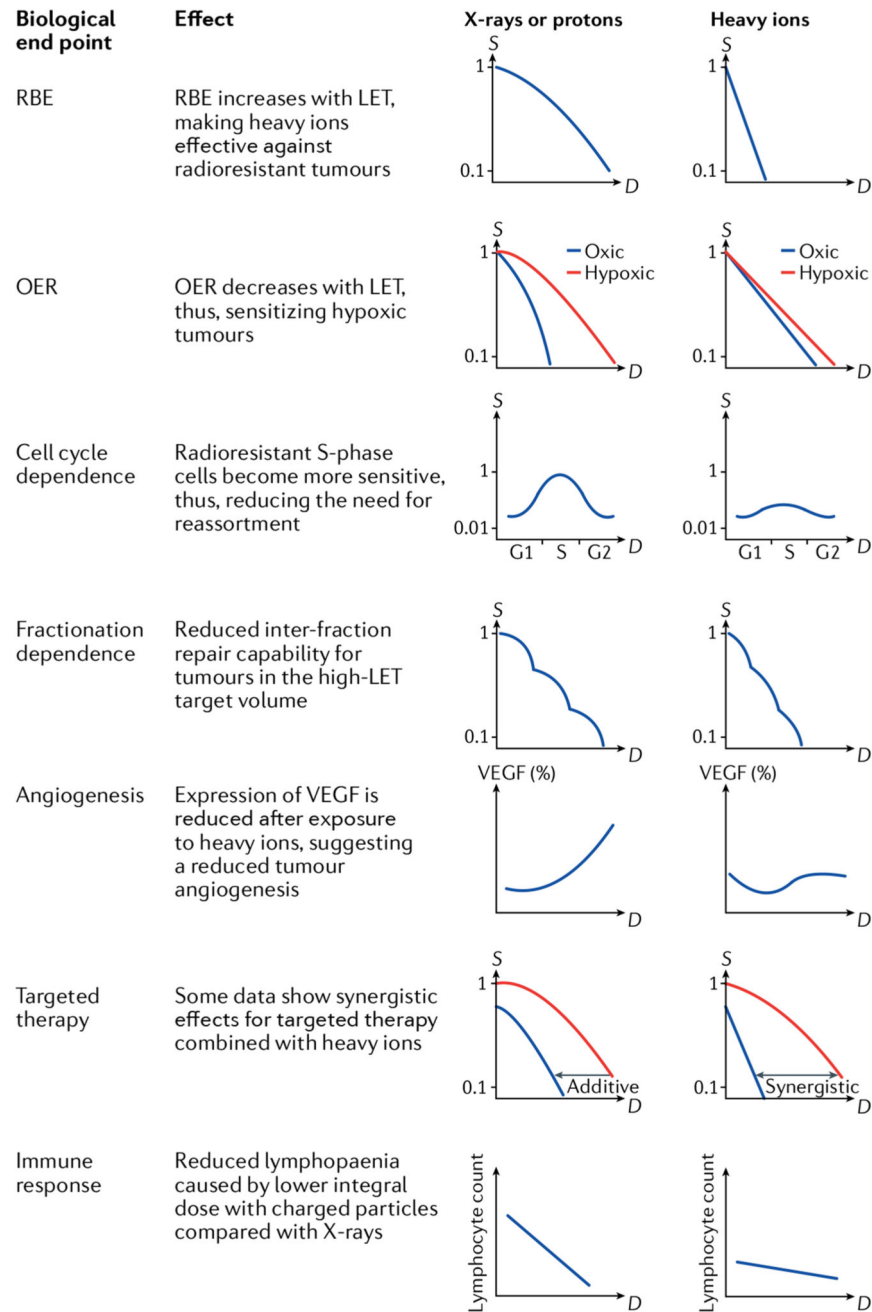


**Figure 5. Biological advantages of heavy ions.**

*D*, dose; G1, pre-DNA replication (S) cell cycle phase; G2, post-DNA replication (S) cell cycle phase; LET, linear energy transfer; OER, oxygen enhancement ratio; RBE, relative biological effectiveness; *S*, survival; VEGF, vascular endothelial growth factor<sup>89</sup>.

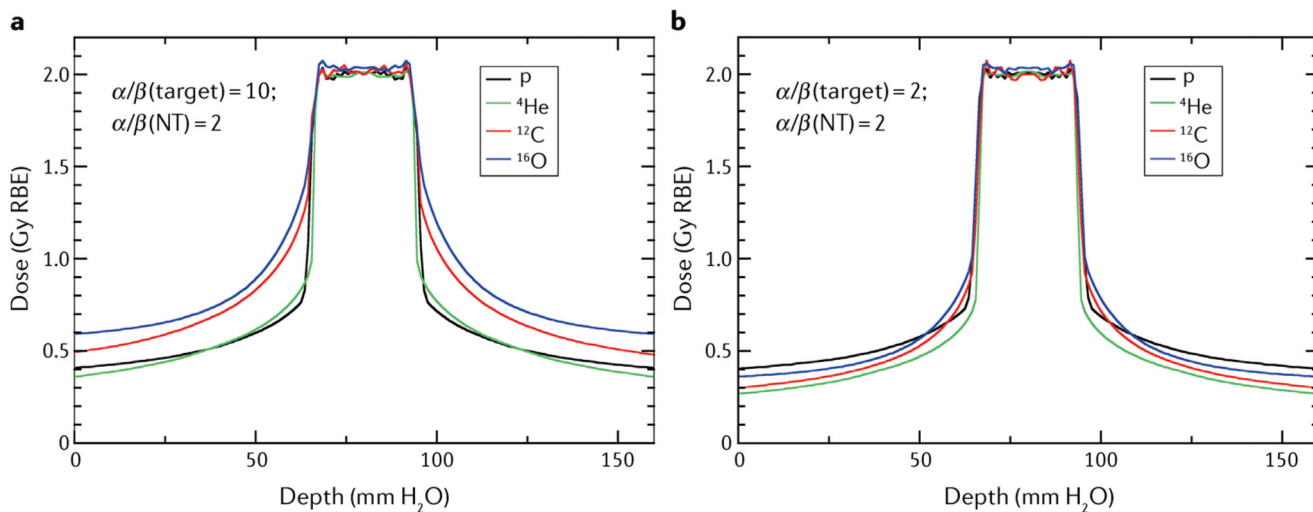


**Figure 6.** The ‘best’ bullets are those providing the lowest relative biological effectiveness-weighted dose in the normal tissue at the same effect in the target.

Relative biological effectiveness (RBE)-weighted dose optimization for a two-opposite-field treatment of an idealized geometry simulating a typical case of radiosensitive (part **a**) or radioresistant (part **b**) tumour. The tumour ( $2.5 \times 2.5 \times 2.5 \text{ cm}^3$ ) is centred in the planning target volume. Biological dose optimization was performed using the TRiP98 software and the local effect model (LEM-IV)<sup>95</sup>. The plan was optimized with different ions to provide the same RBE-weighted dose of 2 Gy in the target volume. Protons are excellent for radiosensitive tumours but the worst for radioresistant tumours. Figure modified from Tommasino et al.<sup>167</sup>, distributed under Creative Commons CC-BY. Figure is adapted from REF.<sup>167</sup>, CC BY 4.0.

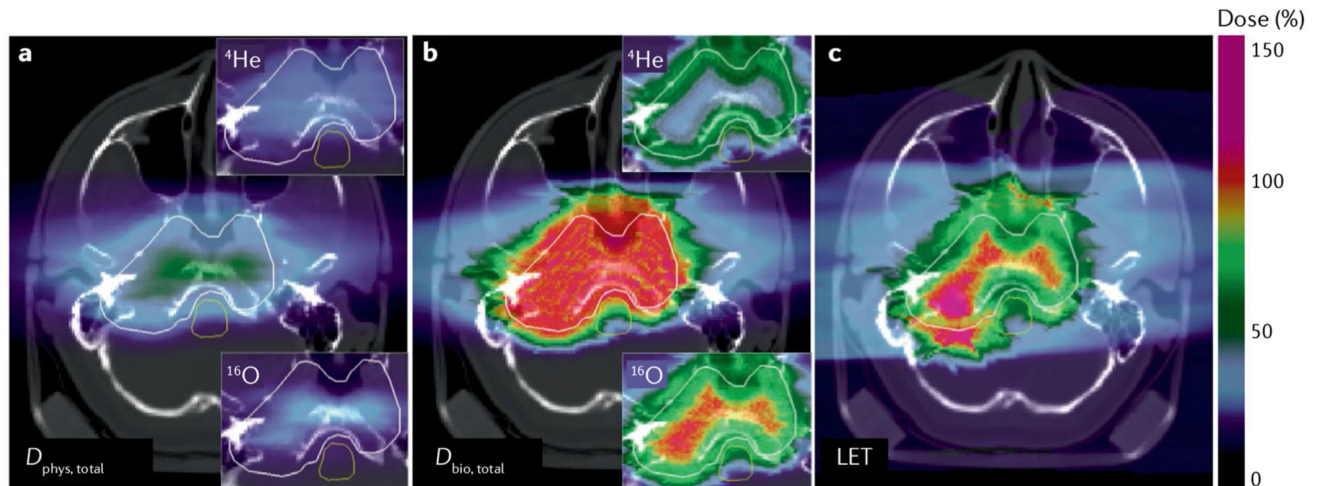


**Figure 7. Biologically optimized multi-ion plan for a hypoxic skull base chordoma (hypoxia is assumed to be concentrated in the central part of the tumour).**

**a** | Total physical dose ( $D_{\text{phys, total}}$ ). Insets correspond to the partial contributions from  $^{16}\text{O}$  and  $^4\text{He}$  fields. Colour scale represents the relative dose compared with the dose of 2 Gy. **b** | Total biological (relative biological effectiveness–oxygen enhancement ratio (RBE–OER)-weighted) dose ( $D_{\text{bio, total}}$ ). Colour scale represents the relative linear energy transfer (LET) compared with a fixed value of  $60 \text{ keV } \mu\text{m}^{-1}$ . **c** | Dose-averaged LET distribution. Colour scale as in part **b**. Calculation with TRiP98 code from Sokol et al.<sup>29</sup>, reproduced with permission from IOP. Figure is adapted from REF.<sup>29</sup>, CC BY 4.0.